Springtime variability of lower tropospheric ozone over Eastern Asia: contributions of cyclonic activity and pollution as observed from space with IASI. Dufour et al.

The authors thank the referees for their interest in the article and their suggestions for improvements.

The comments are addressed below. The referee's comments are indicated in italics and the reply to each comment is given just below. Quoted text from the revised manuscript is given in blue. Following the recommendations of referee #2, major changes have been made in the manuscript, it is then difficult to report all the changes in detail in the response. Please refer to the corrected text provided at the end of the document. An English native speaker has edited the revised version.

Reply to Referee #1:

Specific comments 1:

"1. Validation of IASI against ozonesonde Ozonesonde at Tateno (Tsukuba) are launched in the early afternoon (specifically 14:30LT). Tsukuba site is located in sub-urban area (appox. 50 km away from Tokyo), and there are typically diurnal variations observed, with a maximum in the early afternoon and a minimum during the night due to photochemical build-up and titration by NO, respectively. This means that ozone data by sondes is recorded when lower trop. ozone (say, boundary layer ozone) is at the maximum during the day, resulting in overestimates by sondes versus other methods like UV absorption at the surface sites, when we simply compare daily or monthly means. I think this would be the main cause for the difference between sonde and IASI at Tateno/Tsukuba. I am not familiar with other sites including Beijing, Hong Kong, Naha, and Sapporo, but if the sondes are launched in sub-urban area, we can expect the same bias. In fact, as the authors noted at the footnote of in Table 1, most sonde observations are made in the early afternoon, hence they had to relax time-matching criteria from 6 hr to 24 hr. This can allow the authors to increase the number of matched (concomitant) data, but this does not necessarily contribute to statistical robustness nor improve the validation of IASI against sondes, due to differences in local-time sampling between satellite and sondes, along with substantial diurnal variations at Tsukuba. I would suggest the authors to stick to narrow time band, say 6 hr (by the way, is this +/- 6 hours, correct?) for the sites where diurnal cycles are presumably negligible (say, Naha, Sapporo). This might result in a number that is different from currently estimated (-2DU, -9%) for lower trop. ozone in East Asia.

Also, please specify if "correction factor" is used for ozonesonde in this comparison, and mention the database used here (WOUDC?).

In spite of higher sensitivity of IASI to ozone in the upper atmosphere, the biases for UTLS and STRATO are larger than for LT and TROPO, while correlation coefficients are excellent (0.95). What is the explanation of this?"

Reply:

We follow the recommendation of the referee and keep the 6 hr criterion as coincidence criterion for all the stations including Asian stations. We redo the validation analysis with this criterion for the Asian stations. The number of coincidence is less but similar results are obtained with a negative bias of 2.2 DU and a correlation coefficient of 0.70. Considering each station individually shows a similar large negative bias (2.6 DU) for Beijing, Hong Kong and Tateno whereas the bias is weak for Sapporo (+0.8 DU). We thank the referee to stress the implication of afternoon observation in suburban area like Tateno. The mean time difference between IASI and ozonesondes is ~ +5 hours (IASI measuring in the morning). The difference for Beijing, Hong Kong and Tateno are then explained by this time difference and the build-up of ozone in suburban areas. We include this discussion in the paper as follow: "A significant bias of 2.2 DU (9.5%) with IASI underestimating ozone partial columns is determined. The bias is similar for Beijing, Hong Kong, and Tateno (-2.6 DU) and different for Sapporo (+0.8 DU). Most of the ozonesonde measurements are performed in the early afternoon. The ozone build-up is then maximal in polluted urban or sub-urban sites like Beijing, Hong Kong, and Tateno. IASI observations are performed in the morning, about 5 hours earlier on average. The time difference between IASI and ozonesonde osbervations in polluted suburban sites may partly explain the larger bias in this case. Indeed, the bias for the Sapporo region where the diurnal cycle of ozone is limited is reduced. However, the small number of coincidences does not allow one to firmly conclude on the origin of the observed bias over East Asia."

The WOUDC and the SHADOZ databases have been used to collect the validation dataset except for Aquila and Beijing. This is now mentioned in the corrected version of the paper.

As we focus the validation on the lower troposphere, we do not consider correction factor for the ozonesondes. Applying standard correction factor for tropospheric purposes is usually not recommended (see Chap. 11, p437 of the EUROTRAC report, Tropospheric Ozone Research, Oystein Hov (Editor), Springer, 1997).

Concerning the larger biases for UTLS and STRATO, they are similar to those derived from the previous version of the ozone product and reported in Dufour et al., 2012. The bias in the UTLS has been extensively discussed in this paper. Spectroscopic issues and the limited vertical resolution of IASI, which limits the capability of IASI to retrieve the strong vertical gradient of ozone, mainly explain the biases. Very recently, Boynard et al. (poster presented at the last ESA ATMOS2015 conference, June 2015) show that applying the 2012 version of HITRAN reduces the bias on the total columns (existing when UV and IR sounders are compared). This bias is mainly driven by the stratospheric part of the column. As we focus on the lower troposphere and as the validation results are not significantly different from those discussed in Dufour et al., 2012, we decided not to include the results for the other partial columns and to display the validation results for individual Asian stations instead of all the partial columns.

Specific comments 2:

"2. O3-CO correlation as seen with IASI

In Abstract, the authors mention that they found significant correlation between lower tropospheric ozone and carbon monoxide, especially over North China Plain (NCP), and this O3-CO correlation indicates that the photochemical production of ozone from primary pollutants emitted over such large polluted regions. Later in Page 9217, they mention that the correlation (coefficient?) is 0.6 over NCP for one specific day, 5 May 2008 (Later in Page 9224, the correlation is said as 0.62). The fact that the authors found correlation is good, but more important factor is the slope of O3/CO – i.e., relative enhancement of O3 to CO, as this ratio can suggest the degree of photochemical O3 production per precursor emitted in a given *season of the year. For example, in East Asia, Tanimoto et al. (2008) paper (Tanimoto et al., Diagnosing recent CO emissions and ozone evolution in East Asia using coordinated surface observations, adjoint inverse modeling, and MOPITT satellite data, Atmos. Chem. Phys., 8, 3867-3880, 2008) showed that the O3/CO ratios can vary from 0 to 0.3 as a result of photochemical evolution of the air masses transported from Asian continent. It would be interesting to describe how IASI can see the O3/CO ratios over NCP (and downwind area) and quantitatively discuss the O3/CO ratios in comparison to those in previous papers"*

Reply:

We agree with the referee that looking at the O3/CO ratio would be interesting. At the beginning, we felt reticent about deriving such ratio from IASI. Indeed, the ozone and CO used in the paper are integrated columns on different altitude ranges. The lower tropospheric (LT) columns of ozone are integrated from the surface up to 6 km whereas the CO columns correspond to the total columns. If we retrieve the ozone profile by ourselves, the CO columns used are those available from the Ether atmospheric database (www.pole-ether.fr). Only the columns are distributed (not the profiles). However, assuming that most of the CO enhancement observed from the total CO columns occurs in the lower troposphere, we then calculated the mean mixing ratio corresponding to the LT ozone columns and to the total CO columns to estimate the O3/CO ratios. We computed this ratio only for specific regions (NCP + regions where transport of ozone and CO is observed on 13 and 14 May 2008). The estimated ratios are in the range 0-0.3 given by Tanimoto et al. 2008. During the transported event mentioned in Section 5.4 of the paper, the ratio increases from 0.16 over NCP on 12 May to 0.28 over the Sea of Japan on 14 May, indicating the chemical processing of the transported air masses.

We have then included the following discussion at the end of Section 5.4 of the revised version of the paper: "To complete the study, we calculate the enhancement ratio of O3 to CO over NCP on 12 May, over Yellow Sea and Korea on 13 May, and over the Sea of Japan on 14 May. The ratios are respectively 0.16, 0.21 and 0.28. The increase of the ratio indicates possible photochemical processing during the transport. Part of the large lower tropospheric ozone is then due to the transport of ozone produced over NCP but also to ozone produced during the transport."

We also include the following discussion at the end of Section 4.2: "To evaluate the degree of photochemical production of ozone, we calculate the equivalent or mean mixing ratio corresponding to the CO and LT O3 columns. This allows us to estimate a relative enhancement ratio of O3 to CO of 0.14 and 0.08 on 5 and 6 May respectively. These values are in agreement with the typical values ranging between 0 and 0.3 reported over East Asia by Tanimoto et al. (2008). The estimated enhancement ratio remains quite low suggesting an early stage of ozone production."

The abstract and the conclusion have been updated accordingly.

Specific comments 3:

3. Some other relevant work

P9297, LL27: Wang et al. 2009 paper does not really examine Asian monsoon effect on trop. ozone seasonality, but rather look at long-term trend. Please check. Other relevant references that are missing but dealing with monsoon effect on ozone seasonality (with a focus on *spring) in East Asia is: Tanimoto et al. (2005), Significant latitudinal gradient in the surface ozone spring maximum over East Asia, Geophys. Res. Lett., 32, L21805, doi:10.1029/2005GL023514.*

There is also a paper looking at synoptic-scale transport of air pollutants in East Asia, that the authors might be interested in and add values when discussed in the paper. Miyazaki et al. (2003), Synoptic-scale transport of reactive nitrogen over the western Pacific in spring, J. Geophy. Res., 108(D20), 8788, doi:10.1029/2002JD003248.

Reply:

Indeed, there was an error in the use of the reference Wang et al., 2009. It has been corrected and references to Miyazaki et al. 2003 and Tanimoto et al 2005 have been added in relevant sections of the introduction.

Technical comments

"Title: "contributions" of cyclonic activity and pollution. I found it a bit unfitted to what is discussed in the paper, since "cyclonic activity" is a meteorological factor and "pollution" is a (sort of) source. Perhaps the "role" is better? Or do the authors mean "cyclonic activity on pollution transport"? Anyway it needs to be modified to be clearer."

Reply: the title has been changed as follows: "Springtime daily variations of lower tropospheric ozone over East Asia: role of cyclonic activity and pollution as observed from space with IASI"

"Figure 1 can be omitted since it is not very important and there are as many as 15 figures."

Reply: We removed this figure.

English corrections suggested by the referee have been done.

Reply to Referee #2:

Major comment 1

"In Section 4 and 5, the authors tried to describe the evolution and change of vertical distribution from one synoptic process to the other. There are too many details but lack of key points, which make the paper a bad readability. So I suggest the authors restructure the two sections into two parts. The first part could demonstrate that the IASI satellite data could well-capture the vertical structure of O3 and CO based on correlation analysis with PV or other available data. The secondary part could explain the transport mechanisms for different processes, such as stratospheric intrusion and warm conveyor belt associated with cyclones. The authors should clearly demonstrate what are the unique advantages in using IASI satellite data in understand these processes, and whether there are anything new or anything disagreeing with the existing understanding?"

Reply:

We agree that Sections 4 and 5 are somehow confusing and that the key points are not well underlined. Thanks to the recommendations of the referee, we decided to restructure the paper in order to better state the objectives of the paper and make a better use of the IASI observations.

One objective of the paper is to propose a way to use IASI O3 and CO observations to identify the different sources (UTLS reservoir and photochemical production) of the ozone enhancements in the lower troposphere. The second objective is to evaluate the stratospheric and the photochemical sources of O3 on the daily variations of LT ozone distribution over East Asia using IASI. The main outline of the paper is then to use the first case study to elaborate the analysis method and to apply this method to analyze the second case study. Section 4 is now mainly dedicated to the description of the method based on the first case study and shows (we hope) the potentiality of IASI. We detailed how to use the different partial columns and profiles of ozone to determine (i) the regions under the influence of the tropopause perturbations associated to cyclones, (ii) the regions where STEs occur, (iii) the role of the photochemical production to explain ozone enhancement. We also follow the recommendations of the referee to exploit better the vertical capabilities of IASI (see reply to comment #2). In Section 5, we use this method to discuss the different processing leading to ozone enhancements in the LT with the same sub-sections than previously.

This restructuration of the paper allows us to avoid most of the repetitions, which were in the previous version of the manuscript and also allows us to simplify and reduce the number of figures leading to a better readability (we hope).

To illustrate the new guideline of the paper, we provide here the revised conclusion:

"Based on ozone and CO retrieval from IASI, we elaborate an analysis method to diagnose which processes contribute to ozone enhancement in the lower troposphere. We apply the method to evaluate the respective role of the stratospheric and the photochemical sources of ozone on the day-to-day variation of the lower tropospheric ozone distribution over East Asia. The study allows us to stress how satellite observations can help in monitoring and identifying these different sources. We focus on late springtime because the cyclonic activity – well known to drive the stratosphere-troposphere exchanges – is important and the photochemical production of ozone in polluted area can be significant at this time of the year.

We demonstrate that ozone profiles and semi-independent ozone columns between the surface and 12 km associated with simultaneous CO measurements from IASI provide a powerful observational dataset to identify the stratospheric and anthropogenic origin of lower tropospheric ozone. We show that UT ozone columns larger than 40 DU are a proxy to identify the region of subsiding ozone associated to the tropopause perturbation induced by low-pressure weather systems. Combined with LT ozone columns larger of ~30 DU, it identifies the areas in the lower troposphere affected by the UTLS reservoir of ozone. One of the advantages of IASI is to provide 3 dimensional observations of ozone distribution at synoptic scale when cloud free. The analysis of vertical section in longitude or latitude allows one to identify more precisely the areas where the lower troposphere is connected to the UTLS reservoir and the region of possible irreversible stratosphere-troposphere exchanges. On the contrary, we show that large LT ozone columns when not associated with large UT ozone columns but with enhanced CO total columns – used as pollution tracers – indicates the areas where the photochemical production of ozone takes part of the observed ozone enhancement in the lower troposphere. Once again, the 3D observational capability of IASI (vertical sections) allows one to evaluate if the ozone enhancement observed in the LT is disconnected from the UTLS reservoir and thus to assess the anthropogenic origin of the LT ozone enhancement or the mixing of the sources. We also show that enhancement ratio of O3 to CO, consistent with those from literature, can be derived from IASI.

As expected, the succession of low- and high-pressure systems strongly influences the day-to-day variations of lower tropospheric ozone over North East Asia during springtime, both leading to LT ozone enhancements. We show that the ozone subsiding transfer due to the tropopause perturbations associated with the low-pressure systems affect the free and lower tropospheric ozone over large regions. We determine the region of influence of such system, located mainly above 40°N but with some particular intense events (cut-off low from 11 to 13 May 2008) impacting southern regions such as NCP for few days. The vertical dimension provided by IASI allows the identification of the STE areas, which are located in the southern part behind the cold front in case of frontal system and in the southern or southeastern flank of the low in the case of a cut-off low. Note that the STE are expected to occur preferentially in the western and southern flank of the trough.

Based on the case of a cut-off low travelling over NCP from 11 to 14 May 2008, we show that such systems, with potential convective capacity, when they travel over highly polluted regions, play a key role in the transboundary transport of pollutants. We identify from the O3/CO enhancement ratio estimated from IASI observations that significant ozone photochemical production occurs during the transport from NCP on 12 May to Sea of Japan on 14 May.

In addition to the stratospheric influence on tropospheric ozone in the northern part of the domain, most of the enhanced lower tropospheric ozone columns are observed in regions mainly impacted by strong pollution level. Significant correlations between CO (used as a pollution tracer) and ozone in the lower troposphere have been found. Moreover, the analysis of vertical sections of ozone concentrations over NCP indicates that ozone concentrations are enhanced only in the lower troposphere in such regions, indicating the anthropogenic origin of the observed ozone enhancements. The maximal values of ozone are observed between 2 and 4 km in the cases where an anticyclonic situation is well settled over NCP (e.g. 5 and 15 May 2008). This is in agreement with in situ measurements (Huang et al., 2014), considering the limited vertical resolution of IASI and its limited sensitivity to surface ozone. Because of these limitations, it is not possible to determine more precisely the altitude of the ozone enhancements in the troposphere. This is all the more penalizing when stratospheric and photochemical events occur at the same time. The lack of vertical resolution does not allow one to separate the different contributions. Combined with modelling studies, advanced satellite products coupling UV and IR information such as the recent IASI+GOME-2 product (Cuesta et al., 2013) as well as the next generation of satellite instruments (Crevoisier et al., 2014, Veefkind et al., 2012) should help to address this issue."

Major comment 2

"The vertical sections show some useful information about the structure, which is in fact one of the main unique advantages of satellite data. The authors showed some results in Figure 5 and Figure 11. However, the both figures were show along specific latitudes, and they should

also show results along specific longitudes. In fact, most of works related to stratospheric instructions prefer to a figure along a specific longitude (e.g. Ding and Wang, 2006), which could demonstrate the tropopause folding more clearly."

Reply:

Following the recommendation of the referee, we now provide vertical sections in latitude and in longitude to describe the different events and processes discussed in the paper. We use these vertical sections to evaluate when and where the lower troposphere is connected to the UTLS ozone reservoir and then to identify the areas of possible STE. The vertical distribution of ozone provided by IASI also permits us to identify when ozone enhancements is mainly due to photochemical production from emitted pollutant. We show for example that the ozone distribution retrieved from IASI over NCP during anticyclonic situations shows a maximum between 2 and 4 km in relatively good agreement with in situ observations.

Minor comment 1

"1. The word of "variability" in the title: the paper was not really talk about "variability" but some specific processes. "Variability" is a term related to climatology. The current title will mislead the readers that the cyclonic activity influenced the variability of springtime ozone from year to year."

Reply: The term "variability" has been changed to "variation" in the title and elsewhere in the text.

Minor comment 2

"2. P9205, L5-7, P9209, L5-8: the authors pointed out "May is typically the largest tropospheric ozone along the year". This is not true in East Asia. For example, ozone peaks in June in the NCP and western China and peaks in October in South China (Wang et al., 2009; Ding et al., 2008; Zhu et al., 2004). The reason of selecting May could be that late spring is one of the season having rather high ozone concentration and frequent cyclone/front activities."

Reply: We agree that this statement is misleading. It reads now: "In a previous study, Dufour et al. (2010) show that IASI lower tropospheric ozone columns reach a maximum in late spring, early summer (May, June) in Beijing, Shanghai and Hong Kong. We then decided to focus our study on late spring (May), season for which high ozone concentrations and frequent frontal activities occur over East Asia."

Minor comment 3

"3) Figure 2 and Figure 3: the figures are composed with many small figures. The figure captions are different from the label shows in the figures. For example, (a-c) vs. (a-i) in Figure 2. (a-d) vs. (a-l) in Figure 3. Please make corrections to these figures or capitations, and also check the text."

Reply: The mistake in the figure captions has been corrected and the text checked.

Minor comment 4

“4) A latest work by Ding K. et al. (2015) discussed similar processes using MOZAIC aircraft measurement and MOPITT CO data. Please make a comparison with that paper in the discussion part.”

Reply: A reference to Ding et al. 2015 has been added in the introduction and in section 5.4

Springtime daily variations of lower tropospheric ozone over East Asia: role of cyclonic activity and pollution as observed from space with IASI

G. Dufour[1], M. Eremenko[1], J. Cuesta[1], C. Doche[2], G. Foret[1], M. Beekmann[1], A. Cheiney[3,1], Y. Wang[4], Z. Cai[4], Y. Liu[4], M. Takigawa[5], Y. Kanaya[5], and J.-M. Flaud[1]

[1] {Laboratoire Inter-universitaire des Systèmes Atmosphériques (LISA), UMR7583, Universités Paris-Est Créteil et Paris Diderot, CNRS, Créteil, France}

[2] {Météo France, Direction Inter-Régionale Sud-Ouest, Division Etudes et Climatologie, Mérignac, France}

[3] {Institut National de l'Environnement industriel et des RISques, INERIS, Verneuil-en-Halatte, France}

[4] {Key Laboratory of Middle Atmosphere and Global Environment Observation, Institute of Atmospheric Physics, Chinese Academy of Sciences, Beijing, China}

[5] {Japan Agency for Marine-Earth Science and Technology, Yokohama, Japan}

Correspondence to: G. Dufour (gaelle.dufour@lisa.u-pec.fr)

Abstract

We use satellite observations from IASI (Infrared Atmospheric Sounding Interferometer) on board the MetOp-A satellite to evaluate the springtime daily variations in lower tropospheric ozone over East Asia. The availability of semi-independent columns of ozone from the surface up to 12 km simultaneously with CO columns provides a powerful observational dataset to diagnose the processes controlling tropospheric ozone enhancement at synoptic scales. By combining IASI observations with meteorological reanalyses from ERA-Interim, we elaborate an analysis method based only on IASI ozone and CO observations to identify the respective roles of the stratospheric source and the photochemical source on ozone distribution and variations over East Asia. The succession of low- and high-pressure systems drives the day-to-day variations in lower tropospheric ozone. A case study analysis of one frontal system and one cut-off low system in May 2008 shows that reversible subsiding and

Gaëlle Dufour 15/7/y 13:45
Supprimé: ability

Gaëlle Dufour 6/8/y 17:17
Supprimé: ern

Gaëlle Dufour 15/7/y 13:46
Supprimé: contributions

Gaëlle Dufour 27/8/y 10:57
Supprimé: m

ascending ozone transfers in the upper troposphere lower stratosphere (UTLS) region due to the tropopause perturbations occurring in the vicinity of low-pressure systems impact free and lower tropospheric ozone over large regions, especially north of 40°N, and largely explain the ozone enhancement observed with IASI for these latitudes. Irreversible stratosphere-troposphere exchanges of ozone-rich air masses occur more locally in the southern and south-eastern flanks of the trough. The contribution to the lower tropospheric ozone column is difficult to dissociate from the tropopause perturbations generated by weather systems. For regions south of 40°N, a significant correlation has been found between lower tropospheric ozone and carbon monoxide (CO) observations from IASI, especially over the North China Plain (NCP). Considering carbon monoxide observations as a pollutant tracer, the O_3-CO correlation indicates that the photochemical production of ozone from primary pollutants emitted over such large polluted regions significantly contributes to the ozone enhancements observed in the lower troposphere via IASI. When low-pressure systems circulate over the NCP, stratospheric and pollution sources play a concomitant role in the ozone enhancement. IASI's 3D observational capability allows the areas in which each source dominates to be determined. Moreover, the studied cut-off low system has enough potential convective capacity to uplift pollutants (ozone and CO) and to transport them to Japan. The increase of the enhancement ratio of ozone to CO from 0.16 on 12 May over the North China Plain to 0.28 over the Sea of Japan on 14 May indicates photochemical processing during the plume transport.

1 Introduction

In addition to being an important greenhouse gas (Stevenson et al., 2013), tropospheric ozone (O_3) plays a central role in atmospheric chemistry and air quality, by controlling the oxidation processes through the formation of hydroxyl radicals (OH) (Monks, 2005; Monks et al., 2014). Ozone at high concentrations near the surface is a pernicious pollutant, harmful both to human health and to vegetation (Seinfeld and Pandis, 1997, World Health Organization, 2013). Enhancements of ozone in the mid and lower troposphere result from photochemical production from precursors (NOx and hydrocarbons) and from stratosphere-troposphere exchanges (STE) (Lelieveld and Dentener, 2000). The relative contributions made by these sources depend on the season. It is well established that the peak activity of STE occurs during winter and spring (Monks, 2000) whereas photochemical production is more active

Gaëlle Dufour 6/8/y 14:04
Supprimé: We use satellite observations from IASI (Infrared Atmospheric Sounding Interferometer) on board the MetOp-A satellite to evaluate the springtime daily variability of lower tropospheric ozone at the scale of Eastern Asia. Lower tropospheric partial columns from surface to 6 km are retrieved from IASI with a maximum of sensitivity between 3 and 4 km. We focus our analysis on the month of May 2008 for which tropospheric ozone presents typically amongst the largest concentrations along the year. We combine IASI observations with meteorological reanalyses from ERA-Interim in order to investigate the processes that control the spatial and temporal distribution of lower tropospheric ozone, especially in case of ozone enhancement. The succession of low- and high-pressure systems drives the day-to-day variability of lower tropospheric ozone over North East Asia. The analysis of two episodes with ozone enhancement at the synoptic scale of East Asia shows that the reversible subsiding and ascending ozone transfers in the UTLS region occurring in the vicinity of low-pressure systems and related to tropopause height affect the upper and lower tropospheric ozone over large regions, especially north to 40°N and largely explain the ozone enhancement observed with IASI for these latitudes. Irreversible downward transport of ozone-rich air masses from the UTLS to the lower troposphere occurs more locally. Its contribution to the lower tropospheric ozone column is difficult to dissociate from the tropopause perturbations induced by the weather systems.

Gaëlle Dufour 6/8/y 14:04
Supprimé: to

Gaëlle Dufour 27/8/y 11:01
Supprimé: has been found

Gaëlle Dufour 27/8/y 11:02
Supprimé: with IASI

Gaëlle Dufour 27/8/y 11:03
Supprimé: s

Gaëlle Dufour 6/8/y 14:21
Supprimé: in that case, evidence of pollutant export from NCP towards the east is shown. Finally, we show that semi-independent columns of ozone from the surface up to 12 km associated with CO columns from IASI constitute a powerful observational dataset to investigate the processes controlling tropospheric enhancement of ozone at synoptic scales.

Gaëlle Dufour 27/8/y 11:04
Supprimé: to

Gaëlle Dufour 27/8/y 11:05
Supprimé: of

Gaëlle Dufour 27/8/y 11:05
Supprimé: s

Gaëlle Dufour 27/8/y 11:05
Supprimé: the

during the summer period. The crucial role played by weather systems (cyclonic activity) in determining tropospheric ozone variation has also been well established (e.g. Carmichael et al., 1998; Cooper et al., 1998; Cooper et al., 2002a; Ding et al., 2009). These weather systems are associated with tropopause perturbation, especially low tropopauses, and then with subsiding and ascending ozone transfer in the upper troposphere – lower stratosphere (UTLS) region. In addition, irreversible transfers of ozone can be expected, such as stratosphere-troposphere exchanges that would take place preferentially on the western and southern flanks of the trough (e.g. Ancellet et al., 1994; Holton et al., 1995; Liu et al., 2013), and downward transport from the UTLS to the lower troposphere (e.g. Cooper et al., 2002a). Conceptual models have been proposed to describe airstreams related to traveling low-pressure systems at the midlatitudes (e.g. Cooper et al., 2002b). Two main mechanisms are responsible for part of the ozone temporal and spatial variations observed in the troposphere. The dry airstream (DA) occurring behind cold fronts is responsible for a strong downward transport of ozone from the ULTS down to the middle troposphere. It is often linked to tropopause folding. This downward transport can affect ozone concentrations down to the surface, especially at high altitude sites (e.g. Carmichael et al., 1998; Schuepbach et al., 1999; Dempsey, 2014). In contrast, air masses and then pollutants can be uplifted from the surface to the free troposphere by different processes such as deep convection, orographic lifting and frontal lifting (e.g. Bethan et al., 1998; Hannan et al., 2003; Miyazaki et al., 2003; Cooper et al., 2004, Ding et al., 2009; Foret et al., 2014; Ding et al., 2015, and references therein). One part of these processes, the warm conveyor belts (WCBs) associated with frontal activity and lifting have been studied mainly in the scope of their role in the long-range transport of pollutants, because they lift pollutants to levels where horizontal transport is more efficient. Several studies focusing on the trans-Pacific transport of pollutants from East Asia towards the United States have shown the importance of the frontal systems in this transport process during springtime using both model simulations (e.g. Bey et al., 2001; Liu et al., 2003; Mari et al., 2004; Lin et al., 2010) and dedicated field campaigns (e.g. Jaffe et al., 1999; Cooper et al., 2004; Liang et al., 2004; Oshima et al., 2004). Very recently, Ding et al. (2015) have shown that the topography of East Asia, as well as inducing orographic lifting, assists frontal lifting and facilitates convection, thereby amplifying the possibility of pollutant uplifting.

In recent decades, East Asia and in particular China has experienced rapid economic growth. The related increasing anthropogenic emissions of pollutants (Richter et al., 2005; Lin et al., 2013) lead to regional ozone concentrations amongst the highest in the world (e.g. Chan and

Gaëlle Dufour 27/8/y 11:06
Supprimé:
Gaëlle Dufour 27/8/y 11:06
Supprimé: of
Gaëlle Dufour 27/8/y 11:06
Supprimé: the
Gaëlle Dufour 6/8/y 15:05
Supprimé: variability
Gaëlle Dufour 27/8/y 11:07
Supprimé: i
Gaëlle Dufour 27/8/y 11:07
Supprimé: s
Gaëlle Dufour 28/8/y 11:08
Supprimé: t
Gaëlle Dufour 27/8/y 11:08
Supprimé: On the contrary
Gaëlle Dufour 15/7/y 13:54
Supprimé: warm conveyor belts (WCB) occurring before the cold front allow the transport of air masses and then pollutants from the planetary boundary layer to the free troposphere (
Gaëlle Dufour 27/8/y 11:11
Mis en forme: Non Surlignage
Gaëlle Dufour 27/8/y 11:11
Mis en forme: Non Surlignage
Gaëlle Dufour 6/8/y 15:07
Supprimé: T
Gaëlle Dufour 27/8/y 11:11
Supprimé: under
Gaëlle Dufour 6/8/y 17:23
Supprimé: Since
Gaëlle Dufour 27/8/y 11:13
Supprimé: the past
Gaëlle Dufour 27/8/y 11:13
Supprimé: ve
Gaëlle Dufour 27/8/y 11:13
Supprimé: been
Gaëlle Dufour 27/8/y 11:14
Supprimé: ing a

Yao, 2008; Zhao et al., 2009; Lelieveld and Dentener, 2000; Wang et al., 2012; Safieddine et al., 2013). Due to the rapidly changing emissions in China, the respective contribution made by anthropogenic and natural perturbations to tropospheric ozone in China and its variability constitutes a crucial issue to be documented and better understood. Seasonal variations in ozone levels in East Asia and especially the role of the summer Asian monsoon leading to a summer minimum have been extensively studied from model simulations, in situ and satellite observations (e.g. Mauzerall et al., 2000; Tanimoto et al., 2005; Yamaji et al., 2006; Li et al., 2007; Ding et al., 2008; Dufour et al., 2010). However, at the synoptic scale, the direct impact of weather systems on tropospheric ozone distribution above China and its daily variations has been less extensively considered or, if so, mainly in the scope of the long-range transport of pollutants and export to the Pacific Ocean. A recent study investigates the dynamic and chemical features induced in the upper troposphere by cut-off lows over northeast China using limb and nadir satellite sounders (Liu et al., 2013).

The progress made in satellite observations of tropospheric ozone during the last decade (e.g. Worden et al., 2007; Eremenko et al., 2008; Liu et al., 2010, Nakatani et al., 2012) offers a new opportunity to evaluate ozone distribution and its daily variation including the role of transport at the synoptic scale (e.g. Doche et al., 2014). The satellite provides an unprecedented spatial coverage that allows new insight into how synoptic processes impact ozone distributions. The first satellite measurements of tropospheric ozone were obtained using ultraviolet-visible (UV) sounders (e.g. Fishmann et al., 2003; Liu et al., 2007). Later on, the development of thermal infrared nadir sounders allowed accurate measurements of partial tropospheric ozone columns to be obtained (Coheur et al., 2005; Worden et al., 2007; Dufour et al., 2012; Safieddine et al., 2013). Using GOME and OMI UV sounders, Nakatani et al. (2012) show a persistent belt of enhanced tropospheric columns of ozone at mid-latitudes over East Asia throughout the year, partly attributed to stratospheric intrusion near the subtropical jet. The tropospheric contribution to the enhanced ozone column has been assessed using model simulations. Nakatani et al. (2012) underlined the difficulty in differentiating the stratospheric and tropospheric origins of ozone in the tropospheric columns observed by satellite. This difficulty has already been stated by de Laat et al. (2005). However, it has been demonstrated that thermal infrared sounders like IASI on board MetOp (Clerbaux et al., 2009) allow the retrieval of semi-independent partial columns of ozone within the troposphere (Eremenko et al., 2008; Dufour et al., 2010; Dufour et al., 2012; Safieddine et al., 2013; Barret et al., 2011). Dufour et al. (2010) show the ability of IASI to

Gaëlle Dufour 27/8/y 11:14
Supprimé: of

Gaëlle Dufour 27/8/y 11:15
Supprimé: an

Gaëlle Dufour 27/8/y 11:15
Supprimé: The s

Gaëlle Dufour 27/8/y 11:15
Supprimé: of

Gaëlle Dufour 15/7/y 14:04
Déplacé vers le bas [1]: (e.g. Mauzerall et al., 2000: Yamaji et al., 2006; Li et al., 2007)

Gaëlle Dufour 15/7/y 14:05
Supprimé: (e.g. Ding et al., 2008; Wang et al., 2009)

Gaëlle Dufour 15/7/y 14:04
Déplacé (insertion) [1]

Gaëlle Dufour 15/7/y 14:05
Supprimé: (e.g. Dufour et al., 2010)

Gaëlle Dufour 15/7/y 14:05
Supprimé: :

Gaëlle Dufour 27/8/y 11:16
Supprimé: the

Gaëlle Dufour 27/8/y 11:18
Supprimé: the

Gaëlle Dufour 6/8/y 15:09
Supprimé: variability

Gaëlle Dufour 27/8/y 11:19
Supprimé: under

Gaëlle Dufour 27/8/y 11:19
Supprimé: al

Gaëlle Dufour 6/8/y 15:09
Supprimé: variability

Gaëlle Dufour 28/8/y 10:47
Supprimé: d

Gaëlle Dufour 27/8/y 11:20
Supprimé: was

Gaëlle Dufour 28/8/y 11:38
Supprimé: f

provide independent information on the seasonal variation in lower and upper tropospheric ozone over East Asia. Over shorter-term periods of the order of several days, the retrieved ozone profile with IASI allows the identification of the origin of the observed tropospheric ozone in specific cases. Very recently, Hayashida et al. (2015) show ozone enhancement in the lower troposphere over East Asia using the OMI space-borne ultraviolet spectrometer. They attribute the enhancement mainly to emissions of ozone precursors from open crop residue burning after the winter wheat harvest.

In this paper, we use the IASI observation of lower tropospheric ozone to investigate the influence of synoptic scale weather systems on the distribution of ozone over East Asia. In a previous study, Dufour et al. (2010) show that IASI lower tropospheric ozone columns reach a maximum in late spring and early summer (May, June) in Beijing, Shanghai and Hong Kong. We then decided to focus our study on late spring (May), period during which high ozone concentrations and frequent frontal activities occur over East Asia. We focus on May 2008, as this was the first period available with the new version of the IASI ozone product used for this study. Two case studies associated with travelling low-pressure systems and presenting enhanced ozone in the lower troposphere are analyzed. The first case is used to elaborate the analysis method based on IASI observations of ozone (O_3) and carbon monoxide (CO). We demonstrate that semi-independent ozone columns between the surface and 12 km from IASI associated with simultaneous CO measurements provide a powerful observational dataset to identify, at least partly, the stratospheric and anthropogenic origin of lower free tropospheric ozone. The contributions made by descending air from the UTLS in the vicinity of the weather systems and by the photochemical production of ozone to the enhanced lower tropospheric ozone columns are then investigated for the two case studies.

The paper is structured as follow. In Section 2, the different satellite and meteorological datasets are described. As a new version of the IASI ozone product is used for this study, we provide a summary of the validation of the product with a specific focus on East Asia in Section 3. The analysis method based on ozone and CO columns is detailed in Section 4. Section 5 presents the consequences of a cut-off low travelling over a highly polluted region (North China Plain) in terms of ozone vertical distribution and pollutant transport. A general discussion is given in Section 6 as well as a conclusion in Section 7.

Gaëlle Dufour 7/8/y 14:03
Supprimé: variability

Gaëlle Dufour 27/8/y 11:21
Supprimé: of

Gaëlle Dufour 27/8/y 11:22
Supprimé: ern

Gaëlle Dufour 27/8/y 11:22
Supprimé: n

Gaëlle Dufour 27/8/y 11:22
Supprimé: the

Gaëlle Dufour 15/7/y 14:18
Supprimé: our study

Gaëlle Dufour 15/7/y 14:18
Supprimé: the month of

Gaëlle Dufour 15/7/y 14:22
Supprimé: for which tropospheric ozone presents typically amongst the largest concentrations along the year.

Gaëlle Dufour 27/8/y 11:24
Supprimé: s

Gaëlle Dufour 27/8/y 11:24
Supprimé: s

Gaëlle Dufour 15/7/y 14:31
Supprimé: In the two cases, t

Gaëlle Dufour 27/8/y 11:24
Supprimé: of the

Gaëlle Dufour 27/8/y 11:25
Supprimé: of

Gaëlle Dufour 15/7/y 14:32
Supprimé: based on IASI observations of ozone (O_3) and carbon monoxide (CO) as well as on meteorological indicators. Through these two case studies, we demonstrate that semi-independent ozone columns between the surface and 12 km from IASI associated with simultaneous CO measurements provide a powerful observational dataset to identify, at least partly, the stratospheric and anthropogenic origin of lower free tropospheric ozone. The domain considered in the study as well as some geographical information are given in Fig. 1.

Gaëlle Dufour 15/7/y 14:33
Supprimé: I

Gaëlle Dufour 15/7/y 14:34
Supprimé: s

Gaëlle Dufour 15/7/y 14:34
Supprimé: and 5, the two case studies are presented in details

2 Datasets description

2.1 The IASI instrument

The IASI (Infrared Atmospheric Sounding Interferometer) (Clerbaux et al., 2009) instrument, on board the MetOp-A platform since October 2006, is a nadir-viewing Fourier transform spectrometer. It operates in the thermal infrared between 645 and 2760 cm^{-1} with an apodized resolution of 0.5 cm^{-1}. The field of view of the instrument is composed of a 2 × 2 matrix of pixels with a diameter at nadir of 12 km each. IASI scans the atmosphere with a swath width of 2200 km and crosses the equator at two fixed local solar times 9:30 am (descending mode) and 9:30 pm (ascending mode), allowing the monitoring of atmospheric composition twice a day at any location. The large spectral coverage, high radiometric sensitivity and accuracy, and rather high spectral resolution of the instrument allow this instrument to measure the global distribution of several important atmospheric species (eg. Boynard et al., 2009; George et al., 2009; Clarisse et al., 2011).

Gaëlle Dufour 27/8/y 11:25
Supprimé: r

Gaëlle Dufour 27/8/y 11:25
Supprimé: the

Gaëlle Dufour 27/8/y 11:25
Supprimé: the

2.2 Lower tropospheric ozone from IASI

The IASI ozone profiles and partial columns considered in this paper have been retrieved using the method described in Eremenko et al. (2008). The retrieval is performed using the radiative transfer model KOPRA (Karlsruhe Optimised and Precise Radiative transfer Algorithm) and its inversion module KOPRAFIT (Stiller et al., 2000; Höpfner et al., 2001), both adapted to the nadir-viewing geometry. A constrained least squares fit method with an analytical altitude-dependent regularization is used (Kulawik et al., 2006). The applied regularization method is detailed in Eremenko et al. (2008). To summarize, the regularization matrix is a combination of first order Tikhonov constraints (Tikhonov, 1963) with altitude-dependent coefficients. The coefficients are optimized both to maximize the degrees of freedom (DOF) of the retrieval and to minimize the total error on the retrieved profile. Compared to previous studies using this algorithm (Eremenko et al., 2008; Dufour et al., 2010, 2012), several changes have been made. The emissivity of the surface is now taken into account based on a global monthly IASI-derived climatology (Zhou et al., 2011) allowing a better retrieval above arid regions. Different a priori and constraints are used depending on the tropopause height. This new scheme was introduced to reduce possible compensation effects during the retrieval procedure. An automatic detection of the tropopause height (calculated from the temperature profile retrieved from IASI using the definition based on the

Gaëlle Dufour 27/8/y 11:26
Supprimé: are

Gaëlle Dufour 28/8/y 11:32
Supprimé: 0

lapse rate criterion (WMO, 1957)) has been introduced to discriminate between polar, midlatitudes, and tropical situations. If the tropopause is lower than 10 km, the polar constraint and a priori profile are used. If the tropopause is between 10 and 14 km, the midlatitude constraint and a priori profile are used. If the tropopause is higher than 14 km, the tropical constraint and a priori are used. The midlatitude and tropical regularization matrices are those already used in Eremenko et al. (2008) and Dufour et al. (2010, 2012) respectively. The polar constraint has been specifically developed following the same method as in Eremenko et al. (2008). The a priori profiles are compiled from the ozonesonde climatology of McPeters et al. (2007). The midlatitude a priori profile is set to the climatological profile of the 30-60°N latitude band for summer. The tropical a priori profile is set to the climatological profile of the 10-30°N latitude band over the year. The polar profile is set to the climatological profile of the 60-90°N latitude band for summer. As the version of the ozone product used in this study differs significantly from the version extensively validated in Dufour et al. (2012), a new validation against ozonesondes has been conducted and the results are presented in Section 3. The modifications of the algorithm do not influence the vertical sensitivity of IASI. As shown in Dufour et al. (2010, 2012), two semi-independent partial columns of ozone between the surface and 12 km can be considered: the lower tropospheric column integrating the ozone profile from the surface to 6 km altitude – above sea level (asl) – and the upper tropospheric column integrating the ozone profile from 6 to 12 km altitude. Note that the latter column can include stratospheric air masses depending on the tropopause height. The averaging kernels give information on the vertical sensitivity and resolution of the retrieval. The lower tropospheric column shows a maximum sensitivity typically between 3 and 4 km with a limited sensitivity to the surface (Dufour et al., 2012). This implies that the ozone concentration profile in the lower troposphere is preferentially incremented at these altitudes during the retrieval process, independently if the true ozone profile is perturbed at other altitudes, especially at the surface. Moreover, it is worth noting that the partial columns are only semi-independent which means that they may include partial information from altitudes outside their altitude range. For example, the lower tropospheric column includes information from altitudes higher than its upper limit (6 km). In order to estimate the fraction of contamination of the lower tropospheric column by higher altitudes, we calculated the ratio between the integral of the averaging kernel of the lower tropospheric column from 6 km to 60 km and the integral from the surface to 60 km. Higher atmospheric layers contribute to about 20 to 30 % of the lower tropospheric column in the midlatitude air masses (not shown).

Gaëlle Dufour 27/8/y 11:27
Supprimé: than

Gaëlle Dufour 27/8/y 11:27
Supprimé: significantly

Gaëlle Dufour 27/8/y 11:28
Supprimé: of

Gaëlle Dufour 27/8/y 11:29
Supprimé: . It

Gaëlle Dufour 27/8/y 11:29
Supprimé: by higher altitudes

Note that only the morning overpasses of IASI are considered for this study in order to remain in thermal conditions with a better sensitivity to the lower troposphere.

2.3 Carbon monoxide from IASI

The CO data used here are retrieved from the IASI spectra within the 2143-2181.25 cm^{-1} spectral range using the FORLI-CO retrieval code from the Université Libre de Bruxelles (ULB). FORLI-CO retrievals give CO concentration profiles using the optimal estimation method (Rodgers, 2000) and a single a priori profile. More details are given in Hurtmans et al. (2012). The IASI FORLI-CO product used in this study is the total column, publicly available from the Ether website (http://www.pole-ether.fr). Note that only half of the pixels are available for the year 2008. This explains the difference in measurement density between O_3 and CO observations in the different figures. Carbon monoxide is often used as an indicator of biomass burning and anthropogenic pollution (e.g. Edwards et al., 2004; McMillan et al., 2010). In this study, we use the IASI CO columns as an anthropogenic pollution tracer.

2.4 Meteorological dataset

Meteorological data from the ECMWF ERA-Interim reanalysis are used in our analyses. The reanalysis is based on a 4D-Var assimilation system with a 12-hour analysis window. The spatial resolution of the data set is approximately 80 km on 60 vertical levels from the surface up to 0.1 hPa (Dee et al., 2011). In our analyses, the meteorological parameters are taken at 0:00 UTC, corresponding roughly to the morning overpass time of IASI. The main variables considered in this study are the geopotential height, the potential vorticity (PV), and the horizontal wind field (u and v components), as well as the equivalent potential temperature, the vertical velocity and the convective available potential energy. The geopotential height associated with horizontal wind at 850 hPa give a proxy for describing the weather situation and horizontal transport in the lower troposphere, whereas the same parameters at 300 hPa describe the situation in the UTLS. We also calculate the equivalent potential temperature at 850 hPa and 300 hPa from temperature, relative humidity and specific humidity fields (Bolton, 1980) as an indicator of air masses origin (Holton, 2004). Potential vorticity (PV) is often used as a tracer of tropopause height and of air masses origin (e.g. Bethan et al., 1996). PV values between 1 and 1.6 PVU are representative of the upper troposphere whereas PV values larger than 1.6 PVU are indicators of air mass origin above the dynamical tropopause. In this study, we consider mainly PV averaged at between 300 and 500 hPa with a 50 hPa

Gaëlle Dufour 27/8/y 11:31
Supprimé: the

Gaëlle Dufour 27/8/y 11:32
Supprimé: the

Gaëlle Dufour 27/8/y 11:32
Supprimé: the

interval as we are above all interested in the impact of stratospheric air masses on the free troposphere. In order to investigate the ascending motion of air masses, especially from the boundary layer towards the free troposphere within weather systems, we examine the vertical velocity at different pressure levels as well as the convective available potential energy (CAPE), which informs on the capability of the low-pressure system to vertically transport air masses by convection.

3 Validation of IASI lower tropospheric ozone

Significant changes in the ozone retrieval procedure compared to the validation exercise reported in Dufour et al. (2012) have been made as described in Section 2.2. A new validation exercise was done to evaluate the new version of the ozone product. We use a database of ozonesonde measurements from 2007 to 2012 including 27 stations in the midlatitudinal band (30-60°) in both hemispheres and 16 stations in the tropical band (30°S-30°N). Most of the ozonesonde measurements are from the WOUDC (http://woudc.org/) and SHADOZ (http://croc.gsfc.nasa.gov/shadoz/) databases, except for Aquila and Beijing. A list of stations and related information is provided in Table 1. The coincidence criteria used for the validation are 1° around the station, a time difference smaller than 6 hours and a minimum of 10 clear-sky pixels matching these criteria. The results of the comparison between IASI ozone retrievals and ozonesonde measurements are summarized in Table 2. We focus on the lower troposphere and then no correction factor has been applied on ozonesonde measurements. The results for other partial columns are not significantly different compared to the previous version of the product, extensively discussed by Dufour et al. (2012). The bias for the lower tropospheric column (surface to 6 km asl) is small -0.6 DU (-2.8%) and comparable to the bias estimated at the midlatitudes with the previous version of the product (Dufour et al., 2012). The estimated error is about 2.8 DU (14%) with a correlation coefficient of 0.70. Table 2 also summarizes the results for East Asian ozonesonde stations only (Beijing, Hong Kong, Sapporo and Tateno). A significant bias of 2.2 DU (9.5%) with IASI underestimating ozone partial columns is determined. The bias is similar for Beijing, Hong Kong, and Tateno (-2.6 DU) and different for Sapporo (+0.8 DU). Most of the ozonesonde measurements are performed in the early afternoon. The ozone build-up is then maximal in polluted urban or suburban sites like Beijing, Hong Kong, and Tateno. IASI observations are performed in the morning, about 5 hours earlier on average. The time difference between IASI and ozonesonde

Gaëlle Dufour 27/8/y 11:32
Supprimé: mainly

Gaëlle Dufour 27/8/y 11:33
Supprimé: by

Gaëlle Dufour 27/8/y 11:33
Supprimé: to

Gaëlle Dufour 27/8/y 11:33
Supprimé: The

Gaëlle Dufour 27/8/y 11:33
Supprimé: the

Gaëlle Dufour 27/8/y 11:33
Supprimé: the

Gaëlle Dufour 6/8/y 17:24
Supprimé: ive

Gaëlle Dufour 27/8/y 11:34
Supprimé: are

Gaëlle Dufour 15/7/y 15:51
Supprimé: for different partial columns

Gaëlle Dufour 15/7/y 15:56
Supprimé: B

Gaëlle Dufour 15/7/y 15:56
Supprimé: in

Gaëlle Dufour 4/8/y 15:01
Supprimé: estimated

Gaëlle Dufour 15/7/y 15:57
Supprimé: A validation exercise considering

Gaëlle Dufour 15/7/y 15:58
Supprimé: Naha,

Gaëlle Dufour 15/7/y 15:58
Supprimé: indicates a

Gaëlle Dufour 15/7/y 15:58
Supprimé: larger

Gaëlle Dufour 15/7/y 15:59
Supprimé: in the lower troposphere

Gaëlle Dufour 15/7/y 15:59
Supprimé: by about 2 DU (9%)

Gaëlle Dufour 15/7/y 16:12
Supprimé: However, the time coincidence criterion had to be relaxed to 24 hours to allow a more significant number of coincidences between IASI observations and ozonesonde measurements. The larger time difference

observations in polluted suburban sites may partly explain the larger bias in this case. Indeed, the bias for the Sapporo region, where the diurnal cycle of ozone is limited, is reduced. However, the small number of coincidences does not allow any firm conclusion to be reached on the origin of the observed bias over East Asia.

4 Case study of 4-6 May 2008: on the use of IASI O_3 and CO to diagnose the processes influencing the ozone distribution affected by weather systems

An episode of high ozone is observed in the lower troposphere with IASI in North East Asia from 4 to 6 May 2008. This episode is associated with a low-pressure system travelling from Mongolia through North China to the extreme north of Japan. In this section, we investigate how to use the ozone partial columns and profiles and the CO total columns from IASI to diagnose which processes contribute to the ozone enhancement.

4.1 Low-pressure system and associated IASI ozone distribution

Figure 1 describes the meteorological situation of this episode of high ozone. A large cold front extending from Mongolia to South China on 4 May 2008, from North China to the Southern Japanese Islands on 5 May 2008, and moving eastward from Japan on 6 May 2008 characterizes the low-pressure system (Figs. 1a-c). The regions behind the frontal area and north to the polar jet, situated between 35°N and 40°N on these dates (Figs. 1d-f), are strongly influenced by polar air masses with tropopause heights below 9 km (Figs. 1g-i). The 300-500 hPa mean PV values are larger than 1.6 PVU for the same regions, indicating that the upper troposphere is under the influence of lower stratospheric air masses (Figs. 2j-l). The spatial correlation of low tropopauses and large PV values indicates that reversible subsiding ozone transfer affects the upper troposphere in this case. We then expect an ozone enhancement in the upper troposphere for these regions and we will see in the following how IASI describes this ozone enhancement induced by ozone subsidence. The analysis of the upper tropospheric columns shows that IASI observes columns larger than 40 DU in the regions affected by low tropopauses and large PV (Figs 2g-i). A step gradient between 30 and 40 DU is observed in the upper tropospheric ozone distribution reflecting the step gradient in the PV distribution. The very good spatial correlation of the high UT ozone structures with those of high PV leads us to consider that the upper tropospheric columns of ozone retrieved from IASI can be used

Gaëlle Dufour 27/8/y 11:35
Supprimé: s

Gaëlle Dufour 15/7/y 16:26
Supprimé: influence of weather systems on tropospheric ozone distribution

Gaëlle Dufour 15/7/y 16:26
Mis en forme: Indice

Gaëlle Dufour 16/7/y 14:54
Supprimé: Figure 2 describes the meteorological situation for this period. Figure 3 shows the lower and upper tropospheric ozone columns observed with IASI as well as the total CO columns, also observed with IASI, and the PV averaged between 300 and 500 hPa, taken at the coordinates of IASI pixels.

Gaëlle Dufour 16/7/y 14:55
Supprimé: Influence of the l

Gaëlle Dufour 16/7/y 14:55
Supprimé: on the tropospheric

Gaëlle Dufour 16/7/y 16:28
Supprimé: On 4 May 2008, a large cold front associated to the low-pressure system extends from Mongolia to South China (blue line in Fig. 2a). The region over Mongolia behind the cold front and north to the polar jet situated around 40°N that day (Fig. 2d) is strongly influenced by polar air masses, characterized by a tropopause height smaller than 9 km (Fig. 2g). In the same region,

Gaëlle Dufour 16/7/y 16:30
Supprimé: are observed

Gaëlle Dufour 7/8/y 14:21
Supprimé: 3

Gaëlle Dufour 16/7/y 16:32
Supprimé: reveals

Gaëlle Dufour 16/7/y 16:32
Supprimé: the upper troposphere is mainly affected by reversible subsiding ozone transfer

Gaëlle Dufour 16/7/y 16:32
Supprimé: in this case

Gaëlle Dufour 16/7/y 17:51
Supprimé: Upper tropospheric ozone columns (from 6 to 12 km) larger than 40 DU are observed with IASI in the same region (Fig. 3g). The good spatial correlation of these columns with both large PV values and low tropopause height suggests that

as a proxy to determine the regions affected by subsiding ozone from the lower stratosphere. The threshold of 40 DU seems to be relevant for this identification.

The question now is to determine to what extent IASI is able to inform about the low-pressure system's influence on the lower tropospheric ozone distribution. The physical processes, which may affect the lower tropospheric ozone distribution, are (i) the reversible ozone subsidence associated with low tropopause heights, which induces an enhancement of ozone in the upper and free troposphere, and then partly in the lower troposphere; (ii) irreversible stratosphere-troposphere exchanges, which also lead to ozone enhancement. The first process is expected to affect ozone distribution at a synoptic scale whereas the second process is more localized. Figures 2a-c show that lower tropospheric ozone columns larger than 28 DU are observed with IASI in the vicinity of the low with similar spatial patterns to the UT columns and the PV distribution. The observed enhancement in the lower tropospheric column (surface-6km) arises from

- the actual (reversible) transfer of ozone to the free troposphere;
- the definition of the LT columns by itself. The upper boundary of the column is fixed at 6 km. When the tropopause is low (below 9 km), the LT column arithmetically includes layers with upper tropospheric characteristics;
- the limited vertical resolution of the retrieval and the associated smoothing of the vertical profile. As discussed in Section 2.2, the lower tropospheric column is then partly contaminated by ozone outside the column altitude boundaries. This may contribute to an overestimation of the lower tropospheric column. However, it is difficult to estimate this overestimation in our case because no ozonesonde observations were available along the path of the low.

We show with this case study that having the IASI UT and LT ozone columns allows us to determine those regions affected by the subsiding transfer of ozone occurring behind the frontal area and if the lower troposphere is affected. Now, we will examine if and how IASI can be used to characterize irreversible stratosphere-troposphere exchanges (STE). The analysis of the PV distribution at different pressure levels allows the identification of the region in the vicinity of the low where STE occurs. In the case study from 4 to 6 May 2008, we identify two regions with high PV values down to 600 or 500 hPa on the path of the low (not shown): one on the east coast of Korea on 5 May (~39°N, 128°E) and one offshore to the northeast of Tokyo (~39°N, 142.5°E). The STE is situated in the southeast flank of the low-

Gaëlle Dufour 16/7/y 17:52
Supprimé: identify

Gaëlle Dufour 16/7/y 17:52
Supprimé: of enhanced tropospheric ozone associated with low tropopause inside troughs and possibly due to downward transport from the stratosphere

Gaëlle Dufour 4/8/y 15:08
Mis en forme: Paragraphe de liste, Avec puces + Niveau : 1 + Alignement : 0,63 cm + Retrait : 1,27 cm

Gaëlle Dufour 4/8/y 15:08
Mis en forme: Police :Times, 10 pt,

Gaëlle Dufour 17/7/y 11:04
Supprimé: Large lower tropospheric ozone columns (surface to 6 km asl) are also retrieved from IASI for the same region of large PV (Fig. 3a). The low tropopause height in these regions induces an enhancement of ozone in the upper and free troposphere that may partly explain the enhanced lower tropospheric columns observed with IASI. Moreover, a

Gaëlle Dufour 17/7/y 11:05
Supprimé: from

Gaëlle Dufour 17/7/y 11:06
Supprimé: higher altitudes. As the tropopause is low in this region, the atmospheric layers contaminating the lower tropospheric column present lower stratospheric concentrations of ozone and

Gaëlle Dufour 17/7/y 11:06
Supprimé: lead

Gaëlle Dufour 17/7/y 11:06
Supprimé: s

Gaëlle Dufour 17/7/y 11:06
Supprimé: e

Gaëlle Dufour 17/7/y 11:06
Supprimé: this

Gaëlle Dufour 17/7/y 11:07
Supprimé: in the region

Gaëlle Dufour 4/8/y 15:07
Mis en forme: Police :Times, 10 pt, Couleur de police : Automatique, Français

Gaëlle Dufour 17/7/y 11:49
Supprimé: On 5 May 2008, the low-pressure system moves to the East with the associated cold front extending from North China to the Southern Japanese Islands (Fig. 2b). Polar air masses with low tropopauses influence the troposphere north to Korea for latitudes higher than 37°N (Figs. 2e and 2h). Upper tropospheric ozone columns larger than 40 DU (Fig. 3h) as well as lower tropospheric columns larger than 28 DU (Fig. 3b) are observed with IASI in this region. The good spatial correlation between the ozone partial columns and the PV values larger than 1.6 PVU (Fig. 3k) and the tropopause heights lower than 9 km (Fig. 2h) suggest that reversible subsiding ozone transf ... [1]

Gaëlle Dufour 17/7/y 11:49
Supprimé: for

Gaëlle Dufour 17/7/y 11:55
Supprimé: shows that a small area

pressure system, behind and in the southern part of the cold front in the two cases. Figure 3 displays the longitudinal and latitudinal vertical section of ozone at 128°E and 39°N for 5 May (top) and at 142.5°E and 39°N for 6 May (bottom). On 5 May, strong stratospheric intrusion of ozone is observed between 38°N and 39°N, and between 125°E and 130°E. The vertical section at 128°E shows that the free and lower troposphere are still connected to the polar UTLS reservoir that day. On 6 May, a stratospheric intrusion is observed between 36°N and 38°N, and between 140°E and 143°E. The vertical section along 142°E shows that the enhanced ozone in the lower troposphere (below 7 km) is partly disconnected from the polar UTLS reservoir. Backtrajectories performed with the HYSPLIT trajectory model (Draxler and Rolph; Rolph) show that the 3km-altitude air masses located in this area originate from altitudes between 5 and 7 km the day before from North China and Inner Mongolia (Fig. S1). The tropopause height was around 7-8 km on 5 May 2008 for these regions (Fig. 1h). This means that the air masses reaching northeast of Tokyo at 3 km on 6 May have a UTLS origin and transport ozone-rich air into the lower troposphere. Thus, we show that the downward transport from the UTLS affects ozone concentrations in the lower troposphere for specific regions on the southeastern flank of the weather system, whereas the perturbation of the tropopause associated with this system influences upper and lower tropospheric ozone over larger areas in the vicinity of the low.

4.2 Influence of the high-pressure system on tropospheric ozone distribution over the NCP

On 5 May 2008, an anticyclone is forming over Central East China and the North China Plain. The northwesterly winds reaching the NCP change progressively to southwesterly winds from 4 to 6 May with low winds and then a stagnant situation on 5 May (Figs. 1a-c). This, associated with low cloud coverage and then increasing radiation, is a situation favorable to the accumulation of primary pollutants over the NCP and to the photochemical production of ozone due to both local emissions and regional transport of pollutants. The question here is how IASI is able to describe this situation. The CO columns observed with IASI show enhanced values over the NCP on 5 and 6 May (Figs. 2e and 2f). Considering CO as a pollution tracer, enhanced IASI CO columns can be used to evaluate the build-up of pollutants. Concomitantly, lower tropospheric ozone columns as large as 30 DU are observed (Figs. 2b and 2c). A significant spatial correlation (r=0.6) is calculated between CO and lower tropospheric ozone columns for a square region including the NCP (35-41°N, 114-122°E) on

- Gaëlle Dufour 17/7/y 12:38 — **Supprimé:** , sampled with IASI and showing enhanced lower tropospheric ozone, presents PV values larger than 1 PVU down to 600 hPa (Fig. 4a). This suggests that the lower tropospheric column is affected by the downward transport of upper tropospheric air, rich in ozone, within the dry airstream occurring behind the cold front. In the case presented here (Fig. 3b), the downward transport seems more effective in the southeast flank of the low-pressure system. The contribution of the downward transport on lower tropospheric ozone is difficult to assess more precisely from IASI observations due to the limited vertical resolu ... [2]
- Gaëlle Dufour 7/8/y 14:27 — **Supprimé:** 2
- Gaëlle Dufour 27/8/y 11:39 — **Supprimé:** N
- Gaëlle Dufour 17/7/y 12:38 — **Supprimé:** in this case
- Gaëlle Dufour 27/8/y 11:39 — **Supprimé:** to
- Gaëlle Dufour 4/8/y 15:35 — **Déplacé (insertion) [2]**
- Gaëlle Dufour 4/8/y 15:39 — **Supprimé:** inducing cloud free situation and increasing radiation
- Gaëlle Dufour 7/8/y 14:28 — **Supprimé:** 2
- Gaëlle Dufour 4/8/y 15:39 — **Supprimé:** leads to
- Gaëlle Dufour 4/8/y 15:40 — **Supprimé:** both
- Gaëlle Dufour 4/8/y 15:40 — **Supprimé:** to the
- Gaëlle Dufour 4/8/y 15:45 — **Déplacé (insertion) [3]**
- Gaëlle Dufour 4/8/y 15:45 — **Supprimé:** also
- Gaëlle Dufour 7/8/y 14:29 — **Supprimé:** 3
- Gaëlle Dufour 7/8/y 14:29 — **Supprimé:** 3
- Gaëlle Dufour 4/8/y 15:47 — **Supprimé:** L
- Gaëlle Dufour 4/8/y 15:47 — **Supprimé:** over NCP on 5 and 6 May 2008
- Gaëlle Dufour 7/8/y 14:29 — **Supprimé:** 3
- Gaëlle Dufour 7/8/y 14:29 — **Supprimé:** 3
- Gaëlle Dufour 4/8/y 15:45 — **Déplacé vers le haut [3]:** The CO colu ... [3]
- Gaëlle Dufour 4/8/y 15:48 — **Supprimé:** The CO columns observed with ... [4]
- Gaëlle Dufour 4/8/y 15:48 — **Supprimé:** is 0.6

5 May. In addition, the upper tropospheric ozone column does not show enhanced values over the NCP for these 2 days (Figs. 2h and 2i). The analysis of the vertical section of ozone distribution on 5 May shows that the large ozone concentrations in the Beijing region (Fig. 3, ~39°N and ~116°E) and across the NCP are retrieved below 6 km and are disconnected from the UTLS region. The maximal values of ozone are retrieved between 2 and 3 km over Beijing (Fig. 3) in agreement, considering the vertical sensitivity and resolution of IASI, with in situ measurements, which frequently report high ozone concentrations at an altitude of 1.5-2km above Beijing during April-May (Huang et al., 2014). This associated with the correlation with CO suggests that the enhanced ozone observed with IASI is mainly due to the photochemical transformation of primary pollutants emitted over the NCP. To evaluate the degree of photochemical production of ozone, we calculate the equivalent or mean mixing ratio corresponding to the CO and LT O_3 columns. This allows us to estimate a relative enhancement ratio of O_3 to CO of 0.14 and 0.08 on 5 and 6 May respectively. These values are in agreement with the typical values ranging between 0 and 0.3 reported over East Asia by Tanimoto et al. (2008). The estimated enhancement ratio remains quite low suggesting an early stage of ozone production.

5 Case study of 11-16 May 2008: combined contributions of anthropogenic and stratospheric sources over the NCP and pollution transport

A second episode of high ozone is observed in the lower troposphere over the North China Plain (NCP) from 11 to 16 May 2008. This episode is associated with a cut-off low-pressure system forming on 11 May over Inner Mongolia and moving east on subsequent days. From 14 May, the meteorological regime changes over the NCP with warmer air masses settling within an anticyclonic situation. In this section, we examine the influence of the meteorological situation on the distribution of lower and upper tropospheric ozone with a particular focus on the NCP. Figure 4 describes the meteorological situation for the entire period. Figures 5 and 6 display the lower and upper tropospheric ozone columns and the total CO columns observed with IASI.

5.1 11-13 May: NCP under the direct influence of the cut-off low

On 11 May 2008, a cut-off low is forming over Inner Mongolia (Fig. 4a). The cut-off low is not yet completely dissociated from the polar reservoir. A band of upper tropospheric

Gaëlle Dufour 4/8/y 16:44
Supprimé: If one considers CO as a pollution tracer, this strongly suggests the anthropogenic origin of ozone enhancement observed with IASI in the lower troposphere.

Gaëlle Dufour 4/8/y 15:49
Supprimé: this case

Gaëlle Dufour 7/8/y 14:30
Supprimé: 3

Gaëlle Dufour 7/8/y 14:30
Supprimé: 3

Gaëlle Dufour 4/8/y 15:56
Supprimé: The lower troposphere is then not on the direct influence of

Gaëlle Dufour 4/8/y 15:57
Supprimé: as it was the case for the situation discussed in Section 4.1. Figure 5 shows the vertical sections of ozone concentrations for the latitudes of 39°N, 37°N and 35°N on 5 May 2008. At 39° ... [5]

Gaëlle Dufour 4/8/y 15:58
Supprimé: ing

Gaëlle Dufour 7/8/y 14:31
Mis en forme: Indice

Gaëlle Dufour 7/8/y 14:32
Mis en forme: Indice

Gaëlle Dufour 4/8/y 16:00
Supprimé: again the anthropogenic origin ... [6]

Gaëlle Dufour 4/8/y 15:35
Déplacé vers le haut [2]: On 5 May 20 ... [7]

Gaëlle Dufour 5/8/y 12:57
Supprimé: with IASI

Gaëlle Dufour 27/8/y 11:43
Supprimé: to the E

Gaëlle Dufour 27/8/y 11:43
Supprimé: the

Gaëlle Dufour 27/8/y 11:43
Supprimé: after

Gaëlle Dufour 7/8/y 14:33
Supprimé: s

Gaëlle Dufour 7/8/y 14:33
Supprimé: 6 and 7

Gaëlle Dufour 7/8/y 14:33
Supprimé: 8

Gaëlle Dufour 7/8/y 14:33
Supprimé: 9

Gaëlle Dufour 5/8/y 12:58
Supprimé: as well as the total CO column ... [8]

Gaëlle Dufour 7/8/y 14:33
Supprimé: Note that the reader is referred ... [9]

Gaëlle Dufour 5/8/y 12:58
Supprimé: north to the polar jet, which is ... [10]

Gaëlle Dufour 7/8/y 14:34
Supprimé: 6

Gaëlle Dufour 5/8/y 12:58
Supprimé: and 6d

columns larger than 40 DU is observed by IASI between 35°N and 45°N (Fig. 5g). As seen in Section 4, it indicates that the region is under the influence of subsiding ozone. The lower tropospheric ozone columns do not show a clear enhancement for the same latitude band. On that day, subsiding ozone affects only moderately the lower tropospheric ozone.

On 12 May 2008, the cut-off low is well dissociated from the western current and its center reaches the Bohai Sea (Fig. 4b). Upper tropospheric ozone columns larger than 45 DU are retrieved all around the cut-off low. Lower tropospheric ozone columns larger than 32 DU are observed especially in the southwestern part of the low, just above the NCP (Fig. 5b). The analysis of the vertical section of ozone at 117°E (Fig. 7a) shows that the subsiding transfer of ozone due to the tropopause perturbation strongly affects lower tropospheric ozone north of 33°N. At 32°N, the ozone enhancement observed in the lower troposphere is not connected to the UTLS reservoir, suggesting a possible photochemical origin for this enhancement. IASI CO columns are also enhanced in the NCP region and partly correlated with the enhanced ozone columns (Fig. 5e). This indicates that pollution likely plays a concomitant role in the ozone enhancement in that case.

On 13 May 2008, the centre of the cut-off low moves slightly to the East and reaches the Yellow Sea (Fig. 4c). As for the previous day, large upper and lower tropospheric ozone columns are observed with IASI in the vicinity of the low (Figs. 5c and 5i). The two columns are slightly smaller than the day before over the NCP. The analysis of the vertical section of ozone at 115°E (Fig. 7b) shows that the subsiding transfer of ozone due to the tropopause perturbation is less effective than the previous day. Even if the lower tropospheric ozone remains partly connected to the UTLS reservoir north of 33°N, secondary maxima are observed at ~4 km of altitude, suggesting that an additional source of ozone may contribute to the LT ozone enhancement. South of 33°N the ozone enhancement is clearly located in the lower troposphere. The good spatial correlation of LT ozone enhancement and the strong CO enhancement observed all over the NCP (Fig. 5f) confirms that pollution plays a concomitant role in explaining the ozone distribution in the lower troposphere over the NCP for this day.

5.2 14 May: transition from a cyclonic to an anticyclonic situation

On 14 May 2008, the cut-off low shifts to the Sea of Japan (Fig. 4d). A large area including North China, Korea, and reaching Japan shows upper tropospheric columns larger than 40 DU (Fig. 6g), which indicates the region is under the influence of subsiding ozone. Within this

Gaëlle Dufour 7/8/y 14:34
Supprimé: 8…) and associated to a band ... [11]

Gaëlle Dufour 5/8/y 13:01
Supprimé: (Fig. 6e) …nd its center reache ... [12]

Gaëlle Dufour 7/8/y 14:36
Supprimé: 6…). As for the previous day, ... [13]

Gaëlle Dufour 27/8/y 11:46
Supprimé: between …rom a cyclon ... [14]

Gaëlle Dufour 7/8/y 14:38
Supprimé: 7a…). A large area including ... [15]

area, the largest LT ozone columns are observed in an area less extended and situated on the southeastern flank of the low, mainly over the Sea of Japan (Fig. 6a). The lower troposphere is then certainly under the influence of the UTLS.

Over China, an anticyclonic situation starts to develop south of the NCP inducing a change in the wind regime and warmer conditions from 14 May (Fig. 4d). Enhanced CO columns and lower tropospheric ozone columns are retrieved with IASI over the NCP (Figs. 6a and 6d) with moderate UT ozone columns. The analysis of the vertical section of ozone concentrations at 35°N shows that very large ozone concentrations are retrieved for the entire free and upper troposphere in the eastern part of the section (Fig. 7c). This corresponds to the region over the Sea of Japan under the direct influence of the cut-off low and then greatly influenced by the UTLS. The situation is different over the NCP: ozone concentrations in the upper troposphere are moderate and a distinct maximum in the lower troposphere is clearly visible. This, associated with CO enhancement over the NCP in good spatial correlation with LT ozone, indicates that the ozone enhancement observed with IASI over the NCP is of anthropogenic origin and related to the photochemical production of ozone. On that day, the estimated enhancement ratio of O_3 to CO is 0.11 in agreement with the enhancement ratio calculated for the previous case study.

5.3 15-16 May: NCP under anticyclonic influence

On 15 and 16 May 2008, strong enhancements of CO and lower tropospheric ozone are observed with IASI over the entire NCP (Figs. 6b-c and 6e-f). Both CO and O_3 increase compared to the previous day. The anticyclone is firmly settled over China, leading to a stagnant situation with low winds all over the NCP (Fig. 4e). This situation is favorable to the accumulation of pollutant and then to the photochemical production of ozone. Figure 7d shows the vertical section of ozone concentrations retrieved with IASI at 37°N. The ozone enhancement is located below 4 km, especially between 115°E and 116°E, in agreement with the findings of Section 4.2. This, with CO enhancement, indicates that the ozone enhancement is due to photochemical production from pollutants emitted in the NCP. In this case of stronger CO enhancement, the enhancement ratio of O_3 to CO (0.09 on 15 May and 0.06 on 16 May) decreases compared to the previous days.

Gaëlle Dufour 5/8/y 14:18
Supprimé: coincide with the regions presenting low tropopause heights (Fig. 7g). T…he larg ... [16]

Gaëlle Dufour 7/8/y 14:40
Supprimé: to…the NCP inducing a chang ... [17]

Gaëlle Dufour 7/8/y 14:42
Mis en forme: Indice

Gaëlle Dufour 7/8/y 14:43
Supprimé: 9…-c and 69…-f). Both CO ar ... [18]

Gaëlle Dufour 7/8/y 14:45
Mis en forme: Indice

5.4 Evidence of transboundary transport within the cut-off low

On 13 and 14 May, large CO and O_3 columns are retrieved from IASI over the Yellow Sea and over the Sea of Japan on the southern flank of the cut-off low-pressure system (Figs. 5c and 6a). Fairly strong westerly winds are present at 850 hPa in the same region, suggesting a possible advection of air masses from the NCP towards Japan associated with the weather system (Figs. 4c and 4d). In order to assess whether the weather system may have contributed to transporting the pollutants (O_3 and CO), we perform backtrajectories on 13 May for an area south to Korea (Fig. S2). The 3-km air masses originate from the boundary layer over NCP on 11 May. They have been uplifted and transported at an altitude of between 3 and 4 km on subsequent days (Fig. S2). In order to investigate if the pollutant uplifting on 11 May occurs over a region more extended than those shown on Fig. S2, we examined two meteorological variables that indicate possible ascending motion of air masses: the convective available potential energy (CAPE) and the vertical velocity. Figure 8 shows that CAPE is significant on the inside eastern flank of the cut-off low and that negative vertical velocities, i.e., ascending winds, are present from the surface up to 300 hPa (Fig. 8 shows only the vertical velocity at 700 hPa as an example). In addition, backtrajectories performed on 11 May indicate that most of the air masses between 38-40°N and 116-117°E at 3 km originate from the atmospheric layers below 1 km and circulate over the NCP during the previous 24 hours (Fig. S3). This evidences that pollutants (CO and O_3) have been uplifted from the boundary layer into the free troposphere over NCP and then exported towards Japan by the cut-off low. This transport pathway is relatively well known. Very recently, Ding et al. (2015) studied in detail the uplifting and transport of CO in East Asia. They show that the vertical transport of anthropogenic CO originating from the NCP is mainly carried out by frontal lifting associated or not with WCB. They also pointed out the additional topography's role in the CO lifting over the NCP.

To complete the study, we calculate the enhancement ratio of O_3 to CO over NCP on 12 May, over the Yellow Sea and Korea (32-36°N, 122-130°E) on 13 May, and over the Sea of Japan (30-38°N, 128-140°E) on 14 May. The ratios are respectively 0.16, 0.21 and 0.28. The increase of the ratio indicates possible photochemical processing during the transport. Part of the large lower tropospheric ozone is then due to the transport of ozone produced over the NCP but also to ozone produced during the transport.

Gaëlle Dufour 27/8/y 11:53
Supprimé: i

Gaëlle Dufour 7/8/y 14:45
Supprimé: 8

Gaëlle Dufour 7/8/y 14:46
Supprimé: 9

Gaëlle Dufour 7/8/y 14:46
Supprimé: 6

Gaëlle Dufour 7/8/y 14:46
Supprimé: 7a

Gaëlle Dufour 27/8/y 11:53
Supprimé: evaluate if

Gaëlle Dufour 27/8/y 11:54
Supprimé: the

Gaëlle Dufour 27/8/y 11:54
Supprimé: after

Gaëlle Dufour 27/8/y 11:55
Supprimé: n

Gaëlle Dufour 8/8/y 19:24
Supprimé: 13

Gaëlle Dufour 27/8/y 11:55
Supprimé: the

Gaëlle Dufour 8/8/y 19:24
Supprimé: 13

Gaëlle Dufour 7/8/y 14:49
Mis en forme: Indice

Gaëlle Dufour 5/8/y 15:51
Supprimé: We can assume that p

Gaëlle Dufour 5/8/y 15:51
Supprimé: observed

6 Discussion

The succession of low- and high-pressure systems plays a key role in explaining the day-to-day variations of lower tropospheric ozone over North East Asia. In May 2008, 5 events covering 2-3 days each and leading to significant ozone enhancement in the lower troposphere have been identified. In order to evaluate the regions of influence of the frontal and cyclonic activity on the ozone distribution, we calculated monthly means of lower and upper tropospheric ozone columns (Fig. 9). The monthly means are given with a 0.25°x0.25° horizontal resolution. The upper tropospheric ozone columns are the most affected by the ozone subsiding transfer induced by the tropopause perturbations associated with frontal activity. Looking at UT ozone columns larger than 40 DU provides a view of the region of influence of the frontal and cyclonic activity in terms of ozone enhancement. This region is located north of 40°N and extends from Inner Mongolia to North China and the North of Japan. South of 40°N, the influence of the frontal and cyclonic activity on lower tropospheric ozone decreases.

In order to investigate the role of pollution in enhanced lower tropospheric ozone columns observed with IASI, we compare monthly distribution of lower tropospheric ozone columns with the distribution of total CO columns and tropospheric NO_2 columns, often used as anthropogenic sources tracers (Fig.9). The NO_2 tropospheric columns are those observed by the GOME-2 instrument operating on the same satellite platform than the IASI instrument (Boersma et al., 2004) (http://www.temis.nl/airpollution/no2.html). All the regions of continental East Asia (NCP, Sichuan Basin, North China…) showing large NO_2 tropospheric columns and then indicating large anthropogenic sources present large total CO columns and also large lower tropospheric ozone columns (Fig. 9). A correlation of 0.62 over the entire domain between IASI lower tropospheric ozone and IASI total CO suggests that anthropogenic sources significantly contribute to the ozone observed in the lower troposphere with IASI. The North China Plain, Yangtze River Delta (near Shanghai) and Hubei province (Wuhan region) are the regions most impacted by pollution according to the satellite observations. Large lower tropospheric ozone columns are observed over North China corresponding to the industrialised Shenyang-Harbin axis also visible in CO and NO_2 observations (Fig. 9). However, the ozone plume extends more to the west compared to the CO and NO_2 plumes. This may be explained by the influence of the UTLS, which is larger all over the northern part of the domain. Lower tropospheric columns of ozone might also be

Gaëlle Dufour 6/8/y 12:24
Supprimé: The analysis of two case studies involving low-pressure systems in May 2008 shows the importance of the associated tropopause perturbations and the potential associated ozone transfer (downward transport from the upper troposphere within the dry airstream behind the cold front or in the vicinity of cut-off low-pressure systems) in order to explain the large quantities of ozone observed with IASI in the upper troposphere but also in the lower troposphere. The vertical resolution of IASI does not allow a clear discrimination between the different processes involved in such weather systems. However, the two case studies illustrate also the key role of photochemically produced ozone over large polluted regions such as NCP. The ozone enhancement occurs usually in strong coincidence with CO enhancement when anticyclonic conditions settle. Using CO as a pollutant tracer, we can conclude that most of the ozone enhancement observed in this case is due to photo-oxidation of pollutants emitted over NCP. The satellite observations are limited to cloud-free observations or to observations only weakly contaminated by clouds (<15%). The anticyclonic situations are then preferentially sampled due to the low cloud cover in such situations. This does not mean that ozone enhancement associated to pollution occurs only when high-pressure sy ... [19]

Gaëlle Dufour 5/8/y 16:40
Mis en forme: Surlignage

Gaëlle Dufour 5/8/y 16:40
Supprimé: bility

Gaëlle Dufour 8/8/y 19:25
Supprimé: 14

Gaëlle Dufour 5/8/y 16:40
Supprimé: as well as the monthly mean of PV between 300 and 500 hPa (Fig. 15)

Gaëlle Dufour 5/8/y 16:41
Supprimé: ,

Gaëlle Dufour 5/8/y 16:42
Supprimé: and the ozone transfer from the lower stratosphere

Gaëlle Dufour 5/8/y 16:42
Supprimé: ,

Gaëlle Dufour 5/8/y 16:41
Supprimé: and the PV distribution

Gaëlle Dufour 5/8/y 16:43
Supprimé: to

Gaëlle Dufour 5/8/y 16:43
Supprimé: The upper tropospheric ozone column (6 to 12 km) used in this study is well correl ... [20]

Gaëlle Dufour 8/8/y 19:25
Supprimé: 14

Gaëlle Dufour 8/8/y 19:25
Supprimé: 14

Gaëlle Dufour 27/8/y 11:57
Supprimé: the

Gaëlle Dufour 27/8/y 11:57
Supprimé: the

Gaëlle Dufour 8/8/y 19:25
Supprimé: 14

overestimated during the retrieval because the region is partly arid. Indeed, the ozone retrieval can be partly impacted in regions of low emissivity. In the southern part of the domain, enhanced lower tropospheric ozone columns are observed in the Sichuan Basin and Guangdong province in coincidence with enhanced CO and NO_2 columns. In this latter region, closer to the equator, the distance between two successive swaths of IASI increases. Then, the spatial and temporal coverage of IASI decreases and it is then less easy to follow the daily variations of ozone. Moreover, the maximum of sensitivity of IASI ozone retrievals in the tropics is usually higher in altitude around 5 km (Dufour et al., 2012). IASI observations are then less suitable to efficiently monitor pollution in such cases.

7 Conclusion

Based on ozone and CO retrieval from IASI, we elaborate an analysis method to diagnose which processes contribute to ozone enhancement in the lower troposphere. We apply the method to evaluate the respective role of the stratospheric and the photochemical sources of ozone on the day-to-day variation of the lower tropospheric ozone distribution over East Asia. The study allows us to stress how satellite observations can help in monitoring and identifying these different sources. We focus on late springtime because the cyclonic activity – well known to drive the stratosphere-troposphere exchanges – is important and the photochemical production of ozone in polluted areas can be significant at this time of the year.

We demonstrate that ozone profiles and semi-independent ozone columns between the surface and 12 km associated with simultaneous CO measurements from IASI provide a powerful observational dataset to identify the stratospheric and anthropogenic origin of the lower tropospheric ozone. We show that UT ozone columns larger than 40 DU are a proxy to identify the region of subsiding ozone associated with the tropopause perturbation induced by low-pressure weather systems. Combined with LT ozone columns larger of ~30 DU, it identifies the areas in the lower troposphere affected by the UTLS reservoir of ozone. One of the advantages of IASI is to provide 3-dimensional observations of ozone distribution at synoptic scale when cloud free. The analysis of vertical section in longitude or latitude allows one to identify more precisely the areas where the lower troposphere is connected to the UTLS reservoir and the region of possible irreversible stratosphere-troposphere exchanges. On the contrary, we show that large LT ozone columns when not associated with large UT ozone columns but with enhanced CO total columns – used as a pollution tracer – indicate the

Gaëlle Dufour 5/8/y 16:44
Supprimé: , as it is likely the case in the northwestern part of the domain

Gaëlle Dufour 27/8/y 11:58
Supprimé: the

Gaëlle Dufour 5/8/y 16:44
Supprimé: bility

areas where the photochemical production of ozone forms part of the observed ozone enhancement in the lower troposphere. Once again, the 3D observational capability of IASI (vertical sections) allows one to evaluate if the ozone enhancement observed in the LT is disconnected from the UTLS reservoir and thus to assess the anthropogenic origin of the LT ozone enhancement or the mixing of the sources. We also show that enhancement ratio of O_3 to CO, consistent with those from literature, can be derived from IASI.

As expected, the succession of low- and high-pressure systems strongly influences the day-to-day variations in lower tropospheric ozone over Northeast Asia during springtime, both leading to LT ozone enhancements. We show that the ozone subsiding transfer due to the tropopause perturbations associated with the low-pressure systems affect the free and lower tropospheric ozone over large regions. We determine the region of influence of such systems, located mainly above 40°N but with some particular intense events (e.g. cut-off low from 11 to 13 May 2008) impacting southern regions such as the NCP for few days. The vertical dimension provided by IASI allows the identification of the STE areas, which are located in the southern part behind the cold front in the case of the frontal system and on the southern or south-eastern flanks of the low in the case of a cut-off low. Note that the STE are expected to occur preferentially nn the western and southern flanks of the trough.

Based on the case of a cut-off low travelling over the NCP from 11 to 14 May 2008, we show that such systems, with potential convective capacity, when they travel over highly polluted regions, play a key role in the transboundary transport of pollutants. We identify from the O_3/CO enhancement ratio estimated from IASI observations that significant ozone photochemical production occurs during the transport from the NCP on 12 May to the Sea of Japan on 14 May.

In addition to the stratospheric influence on tropospheric ozone in the northern part of the domain, most of the enhanced lower tropospheric ozone columns are observed in regions mainly impacted by strong pollution level. Significant correlations between CO (used as a pollution tracer) and ozone in the lower troposphere have been found. Moreover, the analysis of vertical sections of ozone concentrations over NCP indicates that ozone concentrations are enhanced only in the lower troposphere in such regions, indicating the anthropogenic origin of the observed ozone enhancements. The maximal values of ozone are observed between 2 and 4 km in cases where an anticyclonic situation is well settled over the NCP (e.g. 5 and 15 May 2008). This is in agreement with in situ measurements (Huang et al., 2014), considering the

Gaëlle Dufour 7/8/y 14:58
Mis en forme: Indice

Gaëlle Dufour 6/8/y 11:32
Supprimé: The possibility with IASI to identify contribution from the lower and the upper tropospheric ozone with a large spatial coverage offers new insight on the synoptic processes controlling tropospheric ozone. Indeed, we show that the state-of-the-art IASI ozone product used in this study has good performances in terms of accuracy and precision, especially in the lower troposphere. Validation against ozonesonde measurements shows small biases (-0.6 DU or -2.8 %) and reasonable error estimates (2.8 DU or 14%) for the lower tropospheric ozone columns.

Gaëlle Dufour 6/8/y 11:35
Supprimé: We show evidence that

Gaëlle Dufour 6/8/y 11:35
Supprimé: bility

Gaëlle Dufour 27/8/y 11:59
Supprimé: of

Gaëlle Dufour 7/8/y 14:59
Supprimé: E

Gaëlle Dufour 6/8/y 11:36
Supprimé: ozone transfer from the lower stratosphere to the troposphere occurring in the vicinity of

Gaëlle Dufour 6/8/y 11:37
Supprimé: (e.g. behind cold fronts)

Gaëlle Dufour 6/8/y 11:37
Supprimé: with different examples taken in May 2008

Gaëlle Dufour 6/8/y 11:55
Supprimé: W

Gaëlle Dufour 6/8/y 11:58
Supprimé: also

Gaëlle Dufour 6/8/y 11:55
Supprimé: also a

Gaëlle Dufour 7/8/y 15:00
Mis en forme: Indice

Gaëlle Dufour 6/8/y 12:04
Supprimé: . This suggests

Gaëlle Dufour 6/8/y 12:07
Supprimé:

limited vertical resolution of IASI and its limited sensitivity to surface ozone. Because of these limitations, it is not possible to determine more precisely the altitude of the ozone enhancements in the troposphere. This is all the more penalizing when stratospheric and photochemical events occur at the same time. The lack of vertical resolution does not allow the various contributions to be differentiated. Combined with modelling studies, advanced satellite products coupling UV and IR information such as the recent IASI+GOME-2 product (Cuesta et al., 2013) as well as the next generation of satellite instruments (Crevoisier et al., 2014, Veefkind et al., 2012) should help assessing this issue.

Acknowledgements

We acknowledge the Institut für Meteorologie und Klimaforschung (IMK), Karlsruhe, Germany, for a licence to use the KOPRA radiative transfer model. This study was supported by the French Space Agency - CNES (project ''IASI-TOSCA''). The IASI mission is a joint mission of Eumetsat and the Centre National d'Etudes Spatiales (CNES, France). The IASI L1 data are distributed in near real time by Eumetsat through the Eumetcast system distribution.We acknowledge the Ether CNES/CNRS-INSU database (http://www.pole-ether.fr) for providing access to IASI Level 1 data. We acknowledge the LATMOS/ULB for the provision of IASI CO total columns through the Ehter CNES/CNRS-INSU database. The authors gratefully acknowledge the NOAA Air Resources Laboratory (ARL) for the provision of the HYSPLIT transport and dispersion model and/or READY website (http://www.ready.noaa.gov) used in this publication. We acknowledge the free use of tropospheric NO2 column data from the GOME-2 sensor from www.temis.nl. The ozonesonde data used in this study were mainly provided by the World Ozone and Ultraviolet Data Centre (WOUDC), the Southern Hemisphere Additional Ozonesondes (SHADOZ), and the Global Monitoring Division (GMD) of NOAA's Earth System Research Laboratory and are publicly available (see http://www.woudc.org, http://croc.gsfc.nasa.gov/shadoz, http://www.esrl.noaa.gov/gmd). The authors thank all those responsible for theWOUDC, SHADOZ, and GMD measurements and archives for making the ozonesonde data available.

References

Gaëlle Dufour 6/8/y 12:11
Supprimé: Finally, we show that being able to retrieve semi-independent columns of ozone from the surface up to 12 km and having simultaneously CO columns from IASI provide a powerful dataset to depict the processes controlling tropospheric ozone enhancement at synoptic scales. ... [21]

Gaëlle Dufour 6/8/y 12:12
Supprimé: Due to the limited vertical resolution of IASI and its limited sensitivity to surface ozone

Gaëlle Dufour 6/8/y 12:22
Supprimé: identify on a fine vertical grid the region of influence in altitude of these different sources.

Gaëlle Dufour 6/8/y 12:23
Supprimé: A

Gaëlle Dufour 6/8/y 12:24
Supprimé: improving the vertical observation of lower tropospheric ozone

Gaëlle Dufour 6/8/y 12:23
Supprimé: These observations combined with modelling studies would help identifying these regions.

Ancellet, G., Beekmann, M., and Papayannis, A.: Impact of a cut-off low development on downward transport of ozone in the troposphere, J. Geophys. Res. 99, 3451-3468, 1994.

Barret, B., Le Flochmoen, E., Sauvage, B., Pavelin, E., Matricardi, M., and Cammas, J. P.: The detection of post-monsoon tropospheric ozone variability over south Asia using IASI data, Atmos. Chem. Phys., 11, 9533-9548, doi:10.5194/acp-11-9533-2011, 2011.

Bethan, S., Vaughan, G. and Reid, S. J.: A comparison of ozone and thermal tropopause heights and the impact of tropopause definition on quantifying the ozone content of the troposphere. Q.J.R. Meteorol. Soc., 122: 929–944. doi: 10.1002/qj.49712253207, 1996

Bethan, S., Vaughan, G., Gerbig, C., Volz-Thomas, A., Richer, H., and Tiddeman, D. A. : Chemical air mass differences near fronts, J. Geophys. Res., 103, D11, 13413-13434, 1998.

Bey, I., Jacob, D. J., Logan, J. A., and Yantosca, R. M. : Asian chemical outflow to the Pacific in spring : Origins, pathways, and budgets, J. Geophys. Res., 106, D19, 23097-23113, 2001.

Boersma, K.F., Eskes, H.J. and Brinksma, E.J.: Error Analysis for Tropospheric NO2 Retrieval from Space, J. Geophys. Res., 109, D04311, doi:10.1029/2003JD003962, 2004.

Bolton, D. : The computation of equivalent potential temperature, Mon. Wea. Rev., 108, 1046–1053, 1980.

Boynard, A., Clerbaux, C., Coheur, P.-F., Hurtmans, D., Turquety, S., George, M., Hadji-Lazaro, J., Keim, C., and Meyer-Arnek, J.: Measurements of total and tropospheric ozone from IASI: comparison with correlative satellite, ground-based and ozonesonde observations, Atmos. Chem. Phys., 9, 6255–6271, doi:10.5194/acp-9-6255-2009, 2009.

Carmichael, G. R., Uno, I., Phadnis, M. J., Zhang, Y., and Sunwoo, Y. : Tropospheric ozone production and transport in the springtime in east Asia, J. Geophys. Res., 103,10649-10671, 1998.

Chan, C. K., and Yao, X., Air pollution in mega cities in China, Atmos. Env., 42, 1-42, 2008.

Clarisse, L., R'Honi, Y., Coheur, P.-F., Hurtmans, D., and Clerbaux, C.: Thermal infrared nadir observations of 24 atmospheric gases, Geophys. Res. Lett., 38, L10802, doi:10.1029/2011GL047271, 2011.

Clerbaux, C., Boynard, A., Clarisse, L., George, M., Hadji-Lazaro, J., Herbin, H., Hurtmans, D., Pommier, M., Razavi, A., Turquety, S., Wespes, C., and Coheur, P.-F.: Monitoring of atmospheric composition using the thermal infrared IASI/MetOp sounder, Atmos. Chem. Phys., 9, 6041–6054, doi:10.5194/acp-9-6041-2009, 2009.

Crevoisier, C., C. Clerbaux, V. Guidard, T. Phulpin, R. Armante, B. Barret, C. Camy-Peyret, J.-P. Chaboureau, P.-F. Coheur, L. Crépeau, G. Dufour, L. Labonnote, L. Lavanant, J. Hadji-Lazaro, H. Herbin, N. Jacquinet-Husson, S. Payan, E. Péquignot, C. Pierangelo, P. Sellitto, and C. Stubenrauch, Towards IASI-New Generation (IASI-NG): impact of improved spectral resolution and radiometric noise on the retrieval of thermodynamic, chemistry and climate variables, Atmos. Meas. Tech., 7, 4367-4385, 2014

Coheur, P.-F., Barret, B., Turquety, S., Hurtmans, D., Hadji-Lazaro, J., and Clerbaux, C.: Retrieval and characterization of ozone vertical profiles from a thermal infrared nadir sounder, J. Geophys. Res., 110, D24303, doi:10.1029/2005JD005845, 2005.

Cooper, O. R., Moody, J. L., Davenport, J. C., Oltmans, S. J., Johnson, B. J., Chen, X., Shepson, P. B., and Merrill, J. T. : Influence of springtime weather systems on vertical ozone distribution over three North American sites, J. Geophys. Res., 103, 22001-22013, 1998.

Cooper, O. R., Moody, J. L., Parrish, D. D., Trainer, M., Holloway, J. S., Hübler, G., Fehsenfeld, F. C., and, Stohl, A. : Trace gas composition of midlatitude cyclones over the western North Atlantic Ocean : A seasonal comparison of O_3 and CO, J. Geophys. Res., 107, D7, 4057, 10.1029/2001JD000902, 2002a.

Cooper, O. R., Moody, J. L., Parrish, D. D., Trainer, M., Ryerson, T. B., Holloway, J. S., Hübler, G., Fehsenfeld, F. C., and Evans, M. J. : Trace gas composition of midlatitude cyclones over the western North Atlantic Ocean : A conceptual model, J. Geophys. Res., 107, D7, 4056, doi :10.1029/2001JD000901, 2002b.

Cooper, O. R., Forster C., Parrish, D., Trainer, M., Dunlea, E., Ryerson, T., Hübbler, G., Fehsenfeld, F., Nicks, D., Holloway, J., de Gouw, J., Warneke, C., Roberts, J. M., Flocke, F., and Moody, J. : A case study of transpacific warm conveyor belt transport : Influence of merging airstreams on trace gas import to North America, J. Geophys. Res., 109, D23S08, doi :10.1029/2003JD003624, 2004.

Cuesta, J., Eremenko, M., Liu, X., Dufour, G., Cai, Z., Höpfner, M., von Clarmann, T., Sellitto, P., Foret, G., Gaubert, B., Beekmann, M., Orphal, J., Chance, K., Spurr, R., and Flaud, J.-M.: Satellite observation of lowermost tropospheric ozone by multispectral synergism of IASI thermal infrared and GOME-2 ultraviolet measurements over Europe, Atmos. Chem. Phys., 13, 9675–9693, 2013.

Draxler, R.R. and Rolph, G.D. HYSPLIT (HYbrid Single-Particle Lagrangian Integrated Trajectory) Model access via NOAA ARL READY Website (http://www.arl.noaa.gov/HYSPLIT.php). NOAA Air Resources Laboratory, College Park, MD.

Dee, D. P., Uppala, S. M., Simmons, A. J., Berrisford, P., Poli, P., Kobayashi, S., Andrae, U., Balmaseda, M. A., Balsamo, G., Bauer, P., Bechtold, P., Beljaars, A. C. M., van de Berg, L., Bidlot, J., Bormann, N., Delsol, C., Dragani, R., Fuentes, M., Geer, A. J., Haimberger, L., Healy, S. B., Hersbach, H., Hólm, E. V., Isaksen, L., Kållberg, P., Köhler, M., Matricardi, M., McNally, A. P., Monge-Sanz, B. M., Morcrette, J.-J., Park, B.-K., Peubey, C., de Rosnay, P., Tavolato, C., Thépaut, J.-N., and Vitart, F.: The ERA-Interim reanalysis: configuration and performance of the data assimilation system, Q. J. R. Meteorol. Soc., 137, 553–597, doi:10.1002/qj.828, 2011.

de Laat, A. T. J., Aben, I., and Roelofs, G. J.: A model perspective on total tropospheric O_3 column variability and implications for satellite observations, J. Geophys. Res., 110, D13303, doi:10.1029/2004JD005264, 2005.

Dempsey, F.: Observations of stratospheric O3 intrusions in air quality monitoring data in Ontario, Canada, Atmos. Environ., 98, 111–122, doi:10.1016/j.atmosenv.2014.08.024, 2014.

Ding, A. J., Wang, T., Thouret, V., Cammas, J.-P., and Nédélec, P.: Tropospheric ozone climatology over Beijing: analysis of aircraft data from the MOZAIC program, Atmos. Chem. Phys., 8, 1-13, 2008.

Ding, A., Wang, T., Xue, L., Gao, J., Stohl, A., Lei, H., Jin, D., Ren, Y., Wang, X., Wei, X., Qi, Y., Liu, J., and Zhang, X. : Transport of north China air pollution by midlatitude cyclones : Case study of aircraft measurements in summer 2007, J. Geophys. Res., 114, D08304, doi :10.1029/2008JD011023, 2009.

Ding, K., Liu, J., Ding, A., Liu, Q., Zhao, T. L., Shi, J., Han, Y., Wang, H., and Jiang, F. : Uplifting of carbon monoxide from biomass burning and anthropogenic sources to the free tropopshere in East Asia, Atmos. Chem. Phys., 15, 2843-2866, 2015.

Doche, C., Dufour, G., Foret, G., Eremenko, M., Cuesta, J., Beekmann, M., and Kalabokas, P.: Summertime tropospheric ozone variability over the Meditterranean basin observed with IASI, Atmos. Chem. Phys., 14, 10589-10600, doi:10.5194/acp-14-10589-2014, 2014.

Dufour, G., Eremenko, M., Orphal, J., and Flaud, J.-M.: IASI observations of seasonal and day-to-day variations of tropospheric ozone over three highly populated areas of China: Beijing, Shanghai, and Hong Kong, Atmos. Chem. Phys., 10, 3787-3801, 2010.

Dufour, G., Eremenko, M., Griesfeller, A., Barret, B., LeFlochmoën, E., Clerbaux, C., Hadji-Lazaro, J., Coheur, P.-F., and Hurtmans, D.: Validation of three scientific ozone products retrieved from IASI spectra using ozonesondes, Atmos. Meas. Tech., 5, 611-630, 2012.

Edwards, D. P., Emmons, L. K., Hauglustaine, D. A., Chu, A., Gille, J. C., Kaufman, Y. J., P'etron, G., Yurganov, L. N., Giglio, L., Deeter, M. N., Yudin, V., Ziskin, D. C.,Warner, J., Lamarque, J.- F., Francis, G. L., Ho, S. P., Mao, D., Chan, J., and Drummond, J. R.: Observations of Carbon Monoxide and Aerosol From the Terra Satellite: Northern Hemisphere Variability, J. Geophys. Res. Atmos., 109, D24202, doi:10.1029/2004JD004727, 2004.

Eremenko, M., Dufour, G., Foret, G., Keim, C., Orphal, J., Beekmann, M., Bergametti, G., and Flaud, J.-M.: Tropospheric ozone distributions over Europe during the heat wave in July 2007 observed from infrared nadir spectra recorded by IASI, Geophys. Res. Lett., 35, L18805, doi:10.1029/2008GL034803, 2008.

Fishman, J., Wozniak, A. E., and Creilson, J. K.: Global distribution of tropospheric ozone from satellite measurements using the empirically corrected tropospheric ozone residual technique: Identification of the regional aspects of air pollution, Atmos. Chem. Phys., 3, 893–907, 2003.

Foret, G., Eremenko, M., Cuesta, J., Sellitto, P., Barré, J., Gaubert, B., Coman, A., Dufour, G., Liu, X., Joly, M., Doche, C., and Beekmann, M. : Ozone pollution : what can we see from space ? A case study, J. Geophys. Res. Atmos., 119, 8476–8499, doi:10.1002/2013JD021340, 2014.

George, M., Clerbaux, C., Hurtmans, D., Turquety, S., Coheur, P.-F., Pommier, M., Hadji-Lazaro, J., Edwards, D. P., Worden, H., Luo, M., Rinsland, C., and McMillan,W.: Carbon monoxide distributions from the IASI/METOP mission: evaluation with other space-borne remote sensors, Atmos. Chem. Phys., 9, 8317–8330, doi:10.5194/acp-9-8317-2009, 2009.

Hannan, J. R., Fuelberg, H. E., Crawford, J. H., Sachse, G. W., and Blake D. R. :Role of wave cyclones in transporting boundary layer air to the free troposphere during the spring 2001 NASA/TRACE-P experiment, J. Geophys. Res., 108, D20, 8782, doi :10.1029/2002JD003105, 2003.

Hayashida, S., Liu, X., Ono, A., Yang, K., and Chance, K. : « Observations of ozone enhancment in the lower troposphere over East Asia from space-borne ultraviolet spectrometer, Atmos. Chem. Phys. Discuss., 15, 2013-2054, 2015.

Holton, J. R., Haynes, P. H., McIntyre, M. E., Douglass, A. R., Rood, R. B., and Pfister, L. : Stratosphere-troposphere exchange, Rev. Geophysics, 33, 4, 403-439, 1995.

Holton, J. R. : An introduction to dynamic meteorology, 4th ed., Elsevier, New York, 2004.

Höpfner, M., Blom, C. E., Echle, G., Glatthor, N., Hase, F., and Stiller, G.: Retrieval simulations for MIPAS-STR measurements, edited by: Smith, W. L., IRS 2000: Current Problems in Atmospheric Radiation, Proc. of the Internat. Radiation Symp., St. Petersburg, Russia, 24–29 July 2000, Hampton, Va., DEEPAK Publ., 2001.

Huang, J., Liu, H., Crawford, J. H., Chan, C., Considine, D. B., Zhang, Y., Zheng, X., Zhao, C., Thouret, V., Oltmans, S. J., Liu, S. C., Jones, D. B. A., Steanrod, S. D., and Damon, M. R. : Origin of springtime ozone enhancements in the lower troposphere over Beijing : In situ measurements and model analysis, Atmos. Chem. Phys. Discuss., 14, 32583-32627, 2014.

Hurtmans, D., Coheur, P.-F., Wespes, C., Clarisse, L., Scharf, O., Clerbaux, C., Hadji-Lazaro, J., George, M., and Turquety, S. : FORLI radiative transfer and retrieval code for IASI, JQSRT, 113, 1391-1408, doi:10.1016/j.jqsrt.2012.02.036, 2012.

Jaffe, D., Anderson, T., Covert, D., Kotchenruther, R., Trost, B., Danielson, J., Simpson, W., Berntsen T., Karlsdottir, S., Blake, D., Harris, J., Carmichael, G., and Uno, I. : Transport of Asian air pollution to North America, Geophys. Res. Lett., 26 (6), 711-714, 1999.

Lelieveld, J., and F. J. Dentener : What controls tropospheric ozone ?, J. Geophys. Res., 105, 3531-3551, 2000.

Kulawik, S. S., Osterman, G., Jones, D. B. A., and Bowman, K.W.: Calculation of altitude-dependent Tikhonov constraints for TES nadir retrievals, IEEE T. Geosci. Remote, 44, 1334–1342, 2006.

Li, J., Z. Wang, H. Akimoto, C. Gao, P. Pochanart, and X. Wang (2007), Modeling study of ozone seasonal cycle in lower troposphere over east Asia, J. Geophys. Res., 112, *D22S25*, doi:10.1029/2006JD008209, 2007.

Liang, Q., L. Jaeglé, D. A. Jaffe, P. Weiss-Penzias, A. Heckman, and J. A. Snow, Long-range transport of Asian pollution to the northeast Pacific: Seasonal variations and transport

Gaëlle Dufour 28/8/y 11:31
Mis en forme: Police :12 pt

Gaëlle Dufour 28/8/y 11:31
Mis en forme: Police :12 pt

Gaëlle Dufour 28/8/y 11:32
Mis en forme: Espace Avant : 0 pt

Gaëlle Dufour 28/8/y 11:31
Mis en forme: Police :12 pt

Gaëlle Dufour 28/8/y 11:31
Mis en forme: Police :12 pt

Gaëlle Dufour 28/8/y 11:31
Mis en forme: Police :12 pt

Gaëlle Dufour 28/8/y 11:31
Mis en forme: Police :12 pt

pathways of carbon monoxide, J. Geophys. Res., 109, D23S07, doi:10.1029/2003JD004402, 2004.

Lin, M., Holloway, T., Carmichael, G. R., and Fiore, A. M. : Quantifying pollution inflow and outflow over East Asia in spring with regional and global models, Atmos. Chem. Phys., 10, 4221–4239, 2010

Lin, J., Pan, D., and Zhang, R.-X.: Trend and Interannual Variability of Chinese Air Pollution since 2000 in Association with Socioeconomic Development: A Brief Overview, Atmos. and oceanic science letters, 6, 84−89, 2013.

Liu, H., D. J. Jacob, I. Bey, R. M. Yantosca, B. N. Duncan, and G. W. Sachse, Transport pathways for Asian pollution outflow over the Pacific: Interannual and seasonal variations, J. Geophys. Res., 108(D20), 8786, doi:10.1029/2002JD003102, 2003.

Liu, X., K. Chance, T.P. Kurosu, Improved ozone profile retrievals from GOME data with degradation correction in reflectance, Atmos. Chem. Phys., 7, 1575-1583, 2007.

Liu, X., P. K. Bhartia, K. Chance, R. J. D. Spurr, T. P. Kurosu, Ozone profile retrievals from the Ozone Monitoring Instrument, Atmos. Chem. Phys., 10, 2521-2537, 2010.

Liu, C. X., Liu, Y., Liu, X., and Chance, K. : Dynamical and chemical features of a cutoff low over Noertheast China in July 2007 : Results from satellite measurements and reanalysis, Adv. Atmos. Sci., 30(2), 525-540, doi : 10.1007/s00376-012-2086-8, 2013.

Mari, C., M. J. Evans, P. I. Palmer, D. J. Jacob, and G. W. Sachse, Export of Asian pollution during two cold front episodes of the TRACE-P experiment, J. Geophys. Res., 109, D15S17, doi:10.1029/2003JD004307, 2004.

Mauzerall, D. L., D. Narita, H. Akimoto, L. Horowitz, S. Walters, D. A. Hauglustaine, and G. Brasseur: Seasonal characteristics of tropospheric ozone production and mixing ratios over East Asia: A global three-dimensional chemical transport model analysis, J. Geophys. Res., 105(D14), 17895–17910, doi:10.1029/2000JD900087, 2000.

McMillan, W. W., Pierce, R., Sparling, L. C., Osterman, G., McCann, K., Fischer, M. L., Rappenglueck, B., Newton, R., Turner, D. D., Kittaka, C., Evans, K., Biraud, S., Lefer, B., Andrews, A., and Oltmans, S.:An Observational and modeling strategy to investigate the impact of remote sources on local air quality: A Houston, Texas case study from TEXAQS II, J. Geophys. Res. Atmos., 115, D01301, doi:10.1029/2009JD011973, 2010.

McPeters, R. D., Labow, G. J., and Logan, J. A.: Ozone climatological profiles for satellite retrieval algorithms, J. Geophys. Res., 112, D05308, doi:10.1029/2005JD006823, 2007.

Miyazaki, Y., Kondo, Y., Koike, M., Fuelberg, H. E., Kiley, C. M., Kita, K., Takegawa, N., Sachse, G. W., Flocke, F., Weinheimer, A. J., Singh, H. B., Eisele, F. L., Zondlo, M., Talbot, R. W., Sandholm, S. T., Avery, M. A., and Blake, D. R. : Synoptic-scale transport of reactive nitrogen over the western Pacific in spring, J. Geophys. Res., 108(D20), 8788 , doi :10.1029/2002JD003248, 2003.

Monks, P. S.: A review of the observations and origins of the spring ozone maximum, Atmos. Environ., 34, 3545-3561, 2000.

Monks, P. S.: Gas-phase radical chemistry in the troposphere, Chem. Soc. Rev., 34, 376–395, 2005.

Monks, P. S., Archibald, A. T., Colette, A., Cooper, O., Coyle, M., Derwent, R., Fowler, D., Granier, C., Law, K. S., Stevenson, D. S., Tarasova, O., Thouret, V., von Schneidemesser, E., Sommariva, R., Wild, O., and Williams, M. L. : Tropospheric ozone and its precursirs from the urban to the global scale from air quality to short-lived climate forcer, Atmos. Chem. Phys. Discuss., 14, 32709-32933, 2014.

Nakatani, A., Kondo, S., Hayashida, S., Nagashima, T., Sudo, K., Liu, X., Chance, K., and Hirota, I. : Enhanced mid-latitude tropospheric column ozone over East Asia : Couple effects of stratospheric ozone intrusion and anthropogenic sources, J. Meteor. Soc. Japan, 90 (2), 207-222, 2012.

Oshima, N., Koike, M., Nakamura, H., Kondo, Y., Takegawa, N., Miyazaki, Y., Blake, D. R., Shirai, T., Kita, K., Kawakami, S., and, Ogawa, T. : Asian chemical outflow to the Pacific in late spring observed during the PEACE-B aircraft mission, J. Geophys. Res., 109, D23S05, doi:10.1029/2004JD004976, 2004.

Richter, A., Burrows, J. P., Nub, H., Granier, C., and Niemeier, U.: Increase in tropospheric nitrogen dioxide over China observed from space, Nature, 437, 129-132, 2005.

Rodgers, C. D.: Inverse methods for atmospheric sounding: Theory and practice, vol. 2, World Scientific Publications, Series on Atmospheric, Ocean, Planet. Phys., Singapore, 2000.

Rolph, G.D. Real-time Environmental Applications and Display sYstem (READY) Website (http://www.ready.noaa.gov). NOAA Air Resources Laboratory, College Park, MD.

Gaëlle Dufour 28/8/y 11:13
Supprimé:

Schuepbach, E., Davies, T. D., and Massacand, A. C. : An usual springtime ozone episode at high elevation in the Swiss Alps : contributions both from cross-tropopause exchange and from the boundary layer, Atmos. Environ., 33, 1735-1744, 1999.

Safieddine, S., C. Clerbaux, M. George, J. Hadji-Lazaro, D. Hurtmans, P.-F. Coheur, C. Wespes, D. Loyola, P. Valks, and N. Hao, Tropospheric ozone and nitrogen dioxide measurements in urban and rural regions as seen by IASI and GOME-2, J. Geophys. Res. Atmos., 118, 10,555–10,566, doi:10.1002/jgrd.50669, 2013.

Seinfeld, J. H., and Pandis, S. N.: Atmospheric Chemistry and Physics, from Air Pollution to Climate Change, John Wiley & Sons Inc., Toronto, Canada, 1997.

Stevenson, D. S., Dentener, F. J., Schultz, M. G., Ellingsen, K., van Noije, T. P. C., Wild, O., Zeng, G., Amann, M., Atherton, C. S., Bell, N., Bergmann, D. J., Bey, I., Butler, T., Cofala, J., Collins, W. J., Derwent, R. G., Doherty, R. M., Drevet, J., Eskes, H. J., Fiore, A. M., Gauss, M., Hauglustaine, D. A., Horowitz, L.W., Isaksen, I. S. A., Krol, M. C., Lamarque, J. F., Lawrence, M. G., Montanaro, V., Muller, J. F., Pitari, G., Prather, M. J., Pyle, J. A., Rast, S., 30 Rodriguez, J. M., Sanderson, M. G., Savage, N. H., Shindell, D. T., Strahan, S. E., Sudo, K., and Szopa, S.: Multimodel ensemble simulations of present-day and near-future tropospheric ozone, J. Geophys. Res.-Atmos., 111, doi:10.1029/2005jd006338, 2006.

Stiller, G. P. (ed) with contributions from v. Clarmann, T., Dudhia, A., Echle, G., Funke, B., Glatthor, N., Hase, F., H¨opfner, M., Kellmann, S., Kemnitzer, H., Kuntz, M., Linden, A., Linder, M., Stiller, G. P., and Zorn, S.: The Karlsruhe Optimized and Precise Radiative Transfer Algorithm (KOPRA), vol. FZKA 6487 of Wissenschaftliche Berichte, Forschungszentrum Karlsruhe, Germany, 2000.

Tanimoto, H., Sawa, Y., Matsueda, H., Uno, I., Ohara, T., Yamaji, K., Kurokawa, J., and Yonemura, S.: Significant latitudinal gradient in the surface ozone spring maximum over East Asia, Geophys. Res. Lett., 32, L21805, doi:10.1029/2005GL023514, 2005.

Tanimoto, H., Sawa, Y., Yonemura, S., Yumimoto, K., Matsueda, H., Uno, I., Hayasaka, T., Mukai, H., Tohjima, Y., Tsuboi, K., and Zhang, L.: Diagnosing recent CO emissions and ozone evolution in East Asia using coordinated surface observations, adjoint inverse modelling, and MOPITT satellite data, Atmos. Chem. Phys, 8, 3868-3880, 2008.

Tikhonov, A.: On the Solution of Incorrectly Stated Problems and a Method of Regularisation, Dokl. Acad. Nauk SSSR, 151, 501–504, 1963.

Veefkind, J. P., Aben, I., McMullan, K., Förster, H., de Vries, J., Otter, G., Claas, J., Eskes, H. J., de Haan, J. F., Kleipool, Q., van Weele, M., Hasekamp, O., Hoogeveen, R., Landgraf, J., Snel, R., Tol, P., Ingmann, P., Voors, R., Kruisinga, B., Vink, R., Visser, H., and Levelt, P. F.: TROPOMI on the ESA Sentinel-5 Precursor: A GMES mission for global observations of the atmospheric composition for climate, air quality and ozone layer applications, Remote Sensing of Environnement, 120, 70-83, doi:10.1016/j.rse.2011.09.027, 2012

Wang, Y., Konopka, P., Liu, Y., Chen, H., Müller, R., Plöger, F., Riese, M., Cai, Z., and Lü, D.: Tropospheric ozone trend over Beijing from 2002-2010: ozonesonde measurements and modelling analysis, Atmos. Chem. Phys., 12, 8389-8399, 2012.

WHO: Review of evidence on health aspects of air pollution – REVIHAAP project: final technical report, WHO/Europe, 2013.

WMO: International list of selected and supplementary ships, 3, WMO 47 (WMO/OMM 47, TP. 18), 143 pp., 1957.

Worden, H. M., Logan, J. A., Worden, J. R., Beer, R., Bowman, K., Clough, S. A., Eldering, A., Fisher, B. M., Gunson, M. R., Herman, R. L., Kulawik, S. S., Lampel, M. C., Luo, M., Megretskaia, I. A., Osterman, G. B., and Shephard, M. W.: Comparisons of Tropospheric Emission Spectrometer (TES) ozone profiles to ozonesondes: Methods and initial results, J. Geophys. Res., 112, D03309, doi:10.1029/2006JD007258, 2007.

Yamaji, K., Ohara, T., Uno, I., Tanimoto, H., Kurokawa, J., and Akimoto, H. : Analysis of the seasonal variation of ozone in the boundary layer in East Asia using the Community Multi-scale Air Quality model: What controls surface ozone levels over Japan?, Atmos. Environ., 40, 1856–1868, 2006.

Zhao, C., Wang, Y., and Zeng, T.: East China plains: a “basin” of ozone pollution. Environ. Sci. Tech., 43, 1911, 2009.

Zhou, D. K., A. M. Larar, X. Liu, W. L. Smith, L. L. Strow, P. Yang, P. Schlussel and X. Calbet (2011), Global land surface emissivity retrieved from satellite ultraspectral IR measurements, Geosci. Rem. Sens. IEEE Trans., 49 (4), 1277-1290.

Gaëlle Dufour 28/8/y 11:37
Supprimé: Wang, T., Wei, X. L., Ding, A. J., Poon, C. N., Lam, K. S., Li, Y. S., Chan, L. Y., and Anson, M.: Increasing surface ozone concentrations in the background atmosphere of southern China, 1994-2007, Atmos. Chem. Phys., 9, 6217-6227, 2009.

Table 1. Ozonesonde stations used for the validation. "N days" represents the number of measurements matching the coincidence criteria.

Station	Location		N days	Station	Location		N days
Ankara	39.97°N	32.86°E	50	Tateno	36.10°N	140.10°E	4
Aquila	42.38°N	13.31°E	11	Uccle	50.80°N	4.35°E	390
Barajas	40.47°N	3.58°W	139	Ushuaia	54.85°S	68.31°W	2
Beijing	39.54°N	117.12°E	7	Valentia	51.93°N	10.25°W	33
Bratts Lake	50.20°N	104.70°W	56	Wallops Island	37.90°N	75.70°W	15
Broadmeadows	37.69°S	144.94°E	19				
Churchill	58.74°N	94.07°W	46	Hanoi	21.02°N	105.80°E	16
De Bilt	52.10°N	5.18°E	104	Hilo	19.43°N	155.04°W	62
Edmonton	53.55°N	114.11°W	2	Hong Kong	22.31°N	114.17°E	93
Egbert	44.23°N	79.78°W	57	Irene	25.90°S	28.22°E	4
Goose Bay	53.31°N	60.36°W	98	Java	7.50°S	112.60°E	6
Hohenpeissenberg	47.80°N	11.00°W	319	Kuala Lumpur	2.73°N	101.70°E	5
Huntsville	34.72°N	86.64°W	9	Nairobi	1.27°S	36.80°E	78
Kelowna	49.93°N	119.40°W	124	Naha	26.20°N	127.70°E	0
Lauder	45.04°S	169.68°E	5	Natal	5.49°S	35.80°W	64
Legionowo	52.40°N	20.97°E	133	Pago	14.23°S	170.56°W	13
Lindenberg	52.21°N	14.12°E	148	Panama	7.75°N	80.25°W	2
Macquarie Island	54.50°S	158.94°E	1	Reunion	21.06°S	55.48°E	87
Payerne	46.49°N	6.57°E	389	Samoa	14.23°S	170.56°W	3
Praha	50.01°N	14.45°E	143	San Cristobal	0.92°S	89.60°W	24
Sapporo	43.10°N	141.30°E	12	Santa Cruz	28.46°N	16.26°W	2
Stony Plain	53.55°N	114.11°W	57	Watukosek	7.50°S	112.60°E	16

Table 2. Validation results in the lower troposphere. The bias (IASI-sonde), the RMS and the correlation coefficient (R) are provided for the lower tropospheric column from surface to 6 km (asl). The bias and RMS are given in DU and in percent in parenthesis.

Station	Bias	RMS	R
All stations	-0.6 (2.8)	2.8 (13.7)	0.70
East Asia	-2.2 (-9.5)	2.7 (11.6)	0.70
Beijing	-2.6 (-9.0)	2.6 (9.0)	0.71
Sapporo	0.8 (3.9)	3.9 (19.8)	0.68
Tateno	-2.6 (-12.1)	2.3 (10.8)	0.60
Hong Kong	-2.6 (-10.9)	2.2 (9.6)	0.67

Gaëlle Dufour 6/8/y 15:46
Supprimé: ª

Gaëlle Dufour 6/8/y 15:46
Supprimé: ª

Gaëlle Dufour 6/8/y 15:46
Supprimé: ª

Gaëlle Dufour 6/8/y 15:47
Supprimé: ª

Gaëlle Dufour 6/8/y 15:46
Supprimé: ª

Gaëlle Dufour 6/8/y 15:47
Supprimé: ª The time coincidence criterion is relaxed to 24 hours for the validation dedica ... [22]

Gaëlle Dufour 27/8/y 12:06
Mis en forme: Non Surlignage

Gaëlle Dufour 6/8/y 15:48
Mis en forme ... [23]

Gaëlle Dufour 27/8/y 12:06
Mis en forme: Non Surlignage

Gaëlle Dufour 27/8/y 12:06
Supprimé: different partial columns of ozone. LT:

Gaëlle Dufour 27/8/y 12:06
Mis en forme: Non Surlignage

Gaëlle Dufour 27/8/y 12:06
Supprimé: L

Gaëlle Dufour 27/8/y 12:06
Mis en forme: Non Surlignage

Gaëlle Dufour 27/8/y 12:06
Supprimé: , TROPO: tropospheric column from surface to 11 km, UTLS: column from 8 to ... [24]

Gaëlle Dufour 27/8/y 12:06
Supprimé: the R

Gaëlle Dufour 27/8/y 12:06
Mis en forme: Non Surlignage

Gaëlle Dufour 6/8/y 15:48
Supprimé:
Bias ... [25]

Gaëlle Dufour 7/8/y 16:57

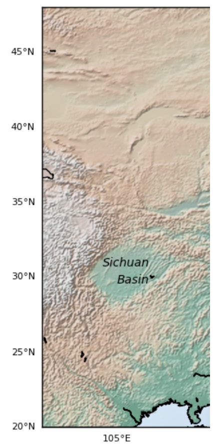

Supprimé:

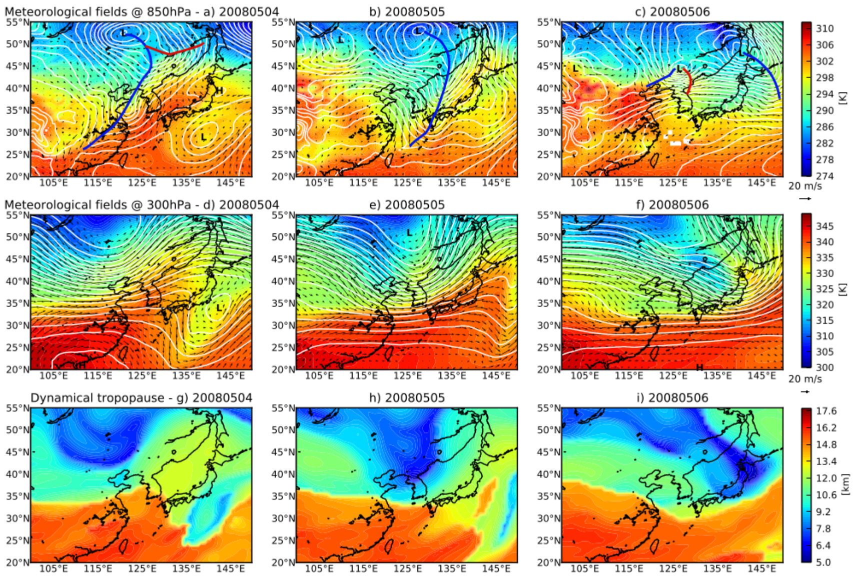

Figure 1. Meteorological situation given at (a-c) 850 hPa and (d-f) 300 hPa from 4 to 6 May 2008 as well as (g-i) the dynamical tropopause. All the meteorological variables are derived from the ERA-Interim reanalysis. The color filled contours in (a-f) represent the equivalent potential temperature and the white contour the geopotential height. The "L" and "H" symbols represent the centre of lows and highs respectively. Horizontal winds are also plotted. The cold and warm fronts are displayed in blue and red respectively on the top panel.

Gaëlle Dufour 7/8/y 16:57
Supprimé: Figure 1. Geographical domain used for the study. ... [26]

Gaëlle Dufour 7/8/y 16:57
Supprimé: 2

Gaëlle Dufour 6/8/y 17:37
Supprimé: b

Gaëlle Dufour 6/8/y 17:37
Supprimé: c

Gaëlle Dufour 27/8/y 12:22
Supprimé: ed

Gaëlle Dufour 6/8/y 17:37
Supprimé: a

Gaëlle Dufour 6/8/y 17:37
Supprimé: and b)

Gaëlle Dufour 27/8/y 12:25
Supprimé: ,

Gaëlle Dufour 27/8/y 12:25
Supprimé: the

Gaëlle Dufour 27/8/y 12:25
Supprimé: The h

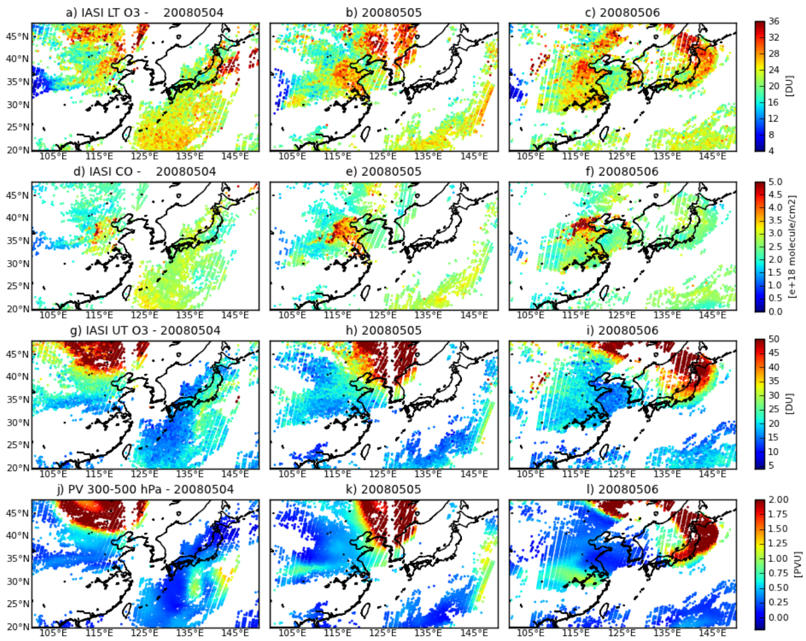

Figure 2. (a-c) Lower tropospheric ozone columns (surface to 6 km asl) retrieved from IASI from 4 to 6 May 2008; (d-f) Total CO columns retrieved from IASI; (g-i) Upper tropospheric ozone columns (6 to 12 km asl) retrieved from IASI; (j-l) Potential Vorticity (PV) from ERA-Interim reanalysis averaged between 300 and 500 hPa.

Gaëlle Dufour 7/8/y 16:57
Supprimé: 3

Gaëlle Dufour 6/8/y 17:37
Supprimé: b

Gaëlle Dufour 6/8/y 17:38
Supprimé: c

Gaëlle Dufour 6/8/y 17:38
Supprimé: d

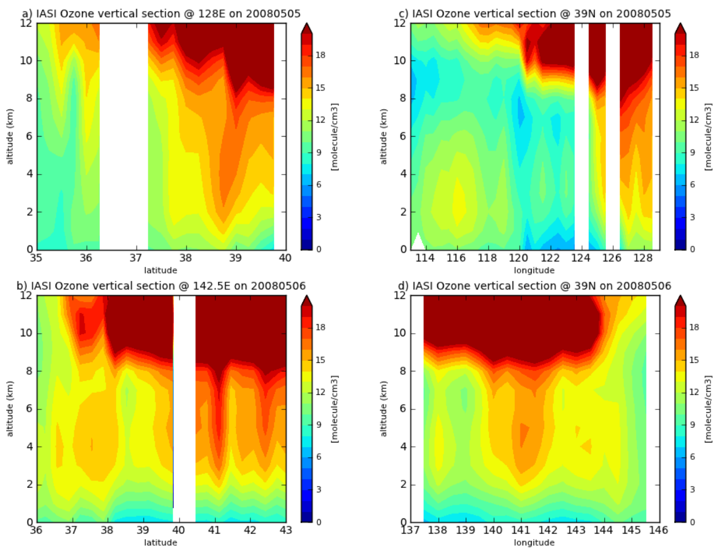

Figure 3. Vertical section of ozone concentration (in molecule/cm^3) retrieved from IASI along specific longitudes – (a) 128°E on 5 May 2008, (b) 142.5°E on 6 May 2008 – and along specific latitudes – 39°N on 5 May 2008 (c) and 6 May 2008 (d). The longitudinal (latitudinal) sections are computed over 1° around the specific longitude (latitude) with a 0.25° resolution in latitude (longitude).

Gaëlle Dufour 7/8/y 16:57

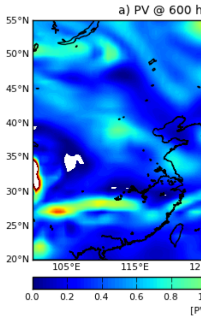

Supprimé:

Gaëlle Dufour 7/8/y 16:57

Supprimé: 4

Gaëlle Dufour 27/8/y 12:10

Mis en forme: Exposant

Gaëlle Dufour 7/8/y 16:57

Supprimé: Potential Vorticity (PV) at 600 hPa from ERA-Interim reanalysis on 5 and 6 May 2008.

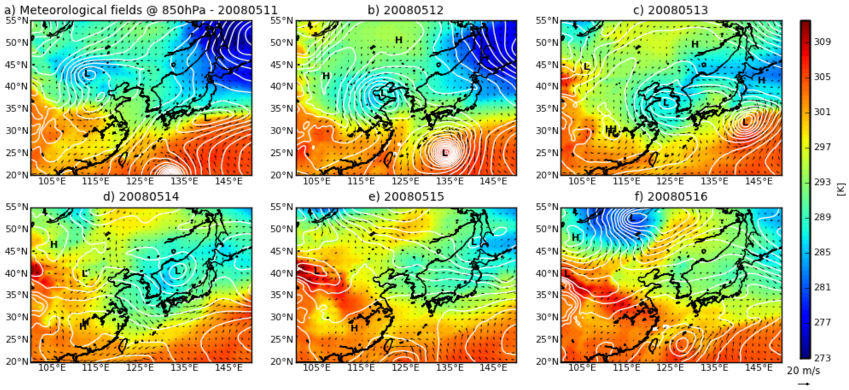

Figure 4. Meteorological situation given at 850 hPa from 11 to 16 May 2008. The color filled contours represent the equivalent potential temperature and the white contour the geopotential height. The "L" and "H" symbols represent the centre of lows and highs respectively. Horizontal winds are also plotted.

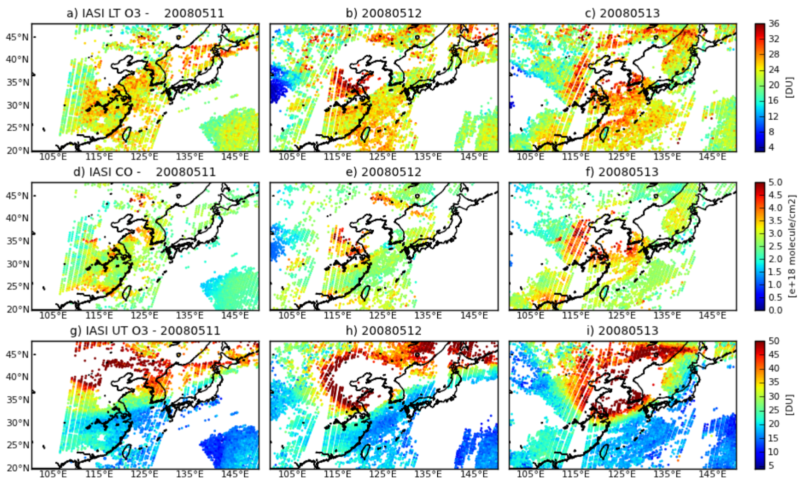

Figure 5. (a-c) Lower tropospheric ozone columns (surface to 6 km a.s.l) retrieved from IASI from 11 to 13 May 2008. (d-f) Total CO columns retrieved from IASI. (g-i) Upper tropospheric ozone columns (6 to 12 km asl) retrieved from IASI.

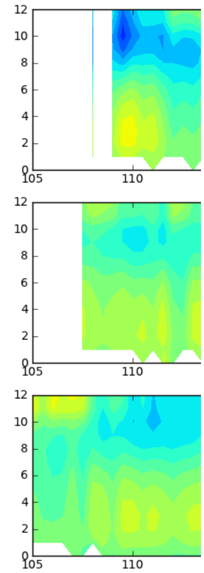

Supprimé:

Gaëlle Dufour 7/8/y 16:58

Supprimé: Figure 5. Vertical section of ozone concentration profiles retrieved with IASI against longitude within 1° latitudinal band at 39°N, 37°N and 35°N on 5 May 2008 ... [27]

Gaëlle Dufour 7/8/y 16:59

Supprimé: 6

Gaëlle Dufour 27/8/y 12:23

Mis en forme: Anglais (E.U.)

Gaëlle Dufour 7/8/y 16:59

Supprimé: same as Fig. 2 for 11 to 13 May 2008.

Gaëlle Dufour 27/8/y 12:23

Mis en forme: Anglais (E.U.)

Gaëlle Dufour 7/8/y 16:59

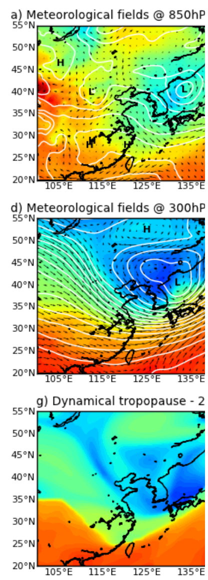

Supprimé:

Gaëlle Dufour 7/8/y 16:59

... [28]

Gaëlle Dufour 7/8/y 16:59

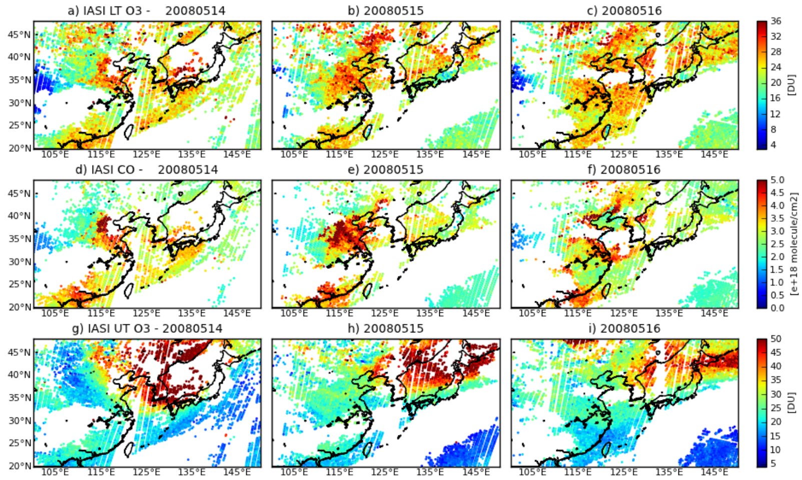

Figure 6. Same as Fig. 6 for 14 to 16 May 2008.

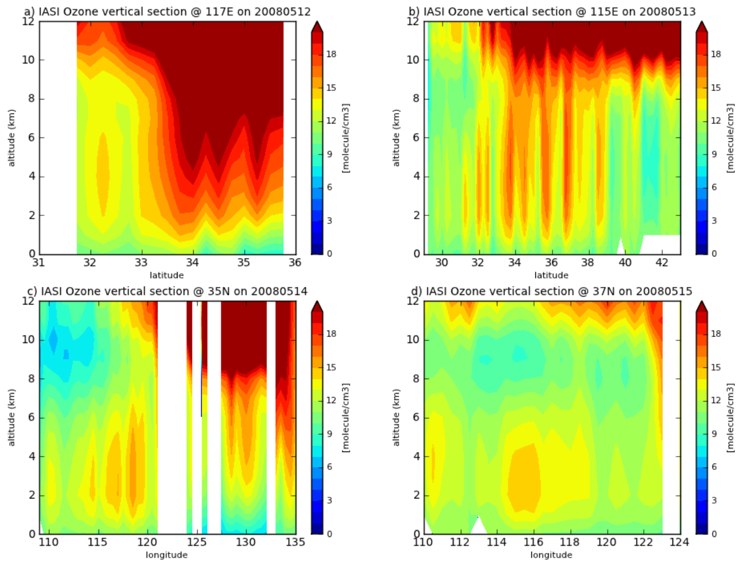

Figure 7. Vertical section of ozone concentration (in molecule/cm^3) retrieved from IASI along specific longitudes – (a) 117°E on 12 May 2008, (b) 115°E on 13 May 2008 – and along specific latitudes – (c) 35°N on 14 May 2008, (d) 37°N on 15 May 2008. The longitudinal

Gaëlle Dufour 7/8/y 16:59

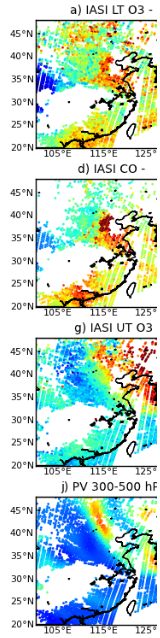

Supprimé:

Gaëlle Dufour 7/8/y 17:00

Supprimé: 9. Same as Fig. 3 for the 14-16 May 2008 period

Gaëlle Dufour 7/8/y 17:00

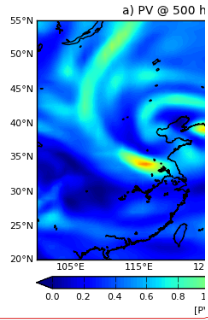

Supprimé:

Gaëlle Dufour 7/8/y 17:00

Supprimé: 10. Potential Vorticity (PV) at 500 hPa from ERA-Interim reanalysis on 12 and 13 May 2008 (latitudinal) sections are computed over 1° around the specific longitude (latitude) with a 0.25° resolution in latitude (longitude).

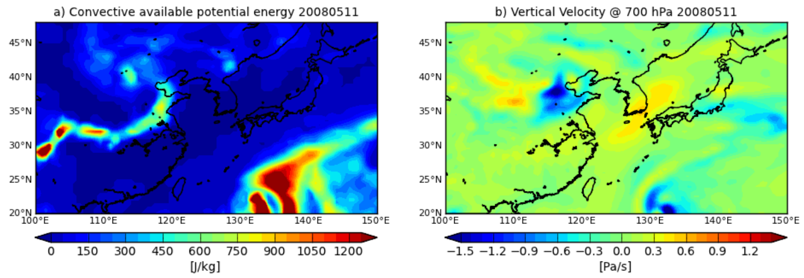

Figure 8. Convective available potential energy (a) and vertical velocity at 700 hPa (b) from ERA-Interim reanalysis.

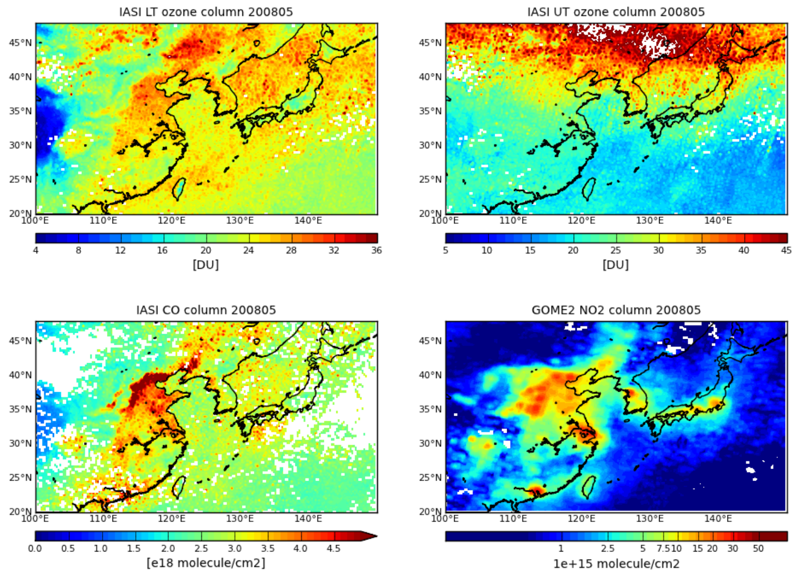

Figure 9. Monthly lower (upper left) and upper (upper right) tropospheric ozone columns observed by IASI in May 2008 as well as monthly IASI total CO columns (lower left) and GOME-2 NO_2 tropospheric columns (lower right) observed in May 2008. The average is calculated for a 0.25°x0.25° resolution grid.

Gaëlle Dufour 27/8/y 17:45
Supprimé: ... [29]

Gaëlle Dufour 7/8/y 17:01
Supprimé: 13

Gaëlle Dufour 27/8/y 17:45
Supprimé:

Gaëlle Dufour 7/8/y 17:01
Supprimé: 14

Supplementary material

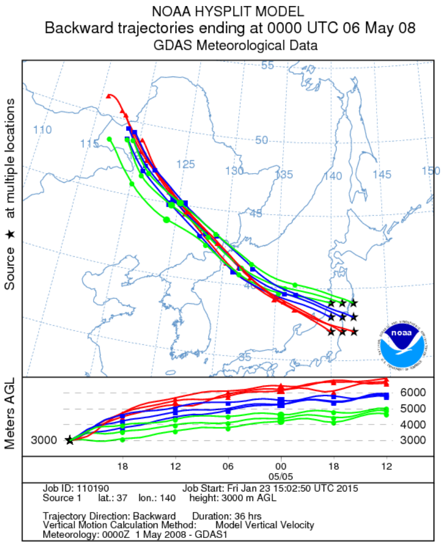

Figure S1. 36-hours backward trajectories ending at 3km on 6 May 2008 in the region of Tokyo.

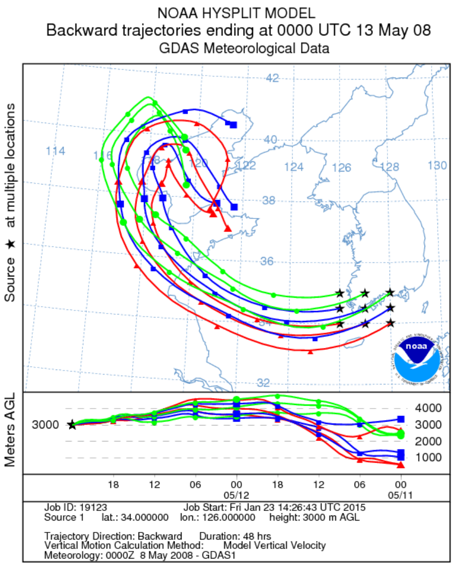

Figure S2. 48-hours backward trajectories ending at 3km on 13 May 2008 in the region of South Korea.

Gaëlle Dufour 8/8/y 19:25

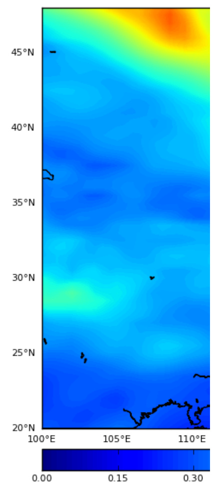

Supprimé: ... [30]

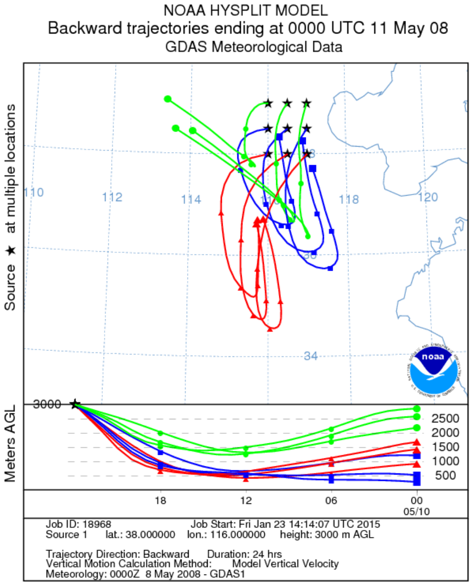

Figure S3. 24-hours backward trajectories ending at 3km on 11 May 2008 in the region of Beijing.